

SERI/PR-234-3012
UC Category 61

**ENTRAINED-FLOW, FAST ABLATIVE PYROLYSIS
OF BIOMASS**

Annual Report
1 December 1984 - 31 December 1985

James P. Diebold
John W. Scahill
Robert J. Evans

July 1986

Prepared Under Task No. 7540.10
Contract No. B-M8108-A-Q

Solar Energy Research Institute
A Division of Midwest Research Institute

1617 Cole Boulevard
Golden, Colorado 80401

Prepared for the
U.S. Department of Energy
Contract No. DE-AC-02-83CH10093

Previous Reports in this Series:

SERI/TP-622-1151
SERI/PR-622-1349
SERI/PR-622-1456
SERI/PR-234-1654
SERI/PR-234-1883
SERI/PR-234-1564
SERI/PR-234-1621
SERI/PR-234-1948
SERI/PR-234-2112
SERI/PR-234-2144
SERI/PR-234-2392
SERI/PR-234-2456
SERI/PR-234-2583
SERI/PR-234-2665

PREFACE

This annual report covers the period of 1 December 1984 through 31 December 1985 for the ablative pyrolysis of biomass in the SERI entrained-flow cyclonic reactor program funded through Pacific Northwest Laboratories operated by Battelle. Dr. Don Jay Stevens is the technical monitor for the program (Contract No. DE-AC-02-83CH10093, Memorandum Purchase Order B-F0409-A-Q). Mr. Simon Friedrich of the Department of Energy's Biomass Energy Technology Division is the program sponsor.



James P. Diebold
Senior Research Chemical Engineer
Thermochemical and Electrochemical
Research Branch



John W. Scahill
Staff Research Chemical Engineer
Thermochemical and Electrochemical
Research Branch



Robert J. Evans
Staff Scientist
Thermochemical and Electrochemical
Research Branch

Approved for

SOLAR ENERGY RESEARCH INSTITUTE



Helena L. Chum
Manager
Chemical Conversion Research Branch



Stan Bull
Director
Solar Fuels Research Division

TABLE OF CONTENTS

	<u>Page</u>
1.0 Introduction.....	1
2.0 Background.....	2
3.0 Vortex Pyrolysis Reactor.....	5
3.1 Pyrolysis System Modifications.....	5
3.2 Pyrolysis Experimentation.....	6
3.3 Summary of Vortex Reactor Effort.....	9
4.0 Zeolite Catalyst Evaluation.....	10
4.1 Introduction.....	10
4.2 Experimental.....	10
4.2.1 Catalyst.....	10
4.2.2 Reactors.....	10
4.2.3 Experiments.....	12
4.3 Projected Product Quality Considerations.....	17
4.4 Maximum Yield Projection.....	17
4.5 Cooperative Agreement with Mobil.....	18
4.6 Zeolite Evaluation Summary.....	18
5.0 Computer Modeling of Biomass Vapor and Hydrocarbon Cracking in a Tubular Reactor.....	19
6.0 Comparison of Computer Model to Experimental Results.....	24
7.0 Summary.....	36
8.0 Future Plans.....	37
9.0 Publications, Presentations, and Formal Education.....	38
10.0 References.....	39

LIST OF FIGURES

	<u>Page</u>
2-1 Schematic of Ablative Pyrolysis System.....	3
4-1 Mass Spectra Showing the Effect of Zeolite Catalysis on Methanol....	13
4-2 Mass Spectra of the Effect of Zeolite Catalyst on Cellulose-Derived Vapors.....	14
4-3 Mass Spectra of Furan over Quartz Wool Blank and Zeolite Catalyst Showing No Major Conversion under Conditions used in These Experiments.....	15
4-4 Mass Spectra of the Primary Pyrolysis of Pine Wood and the Product Distribution After Zeolite Conversion.....	16
6-1 Computer Simulation of Propane Cracking.....	25
6-2 Primary Vapor Cracking Predictions for Simulated Run 55 (650°C), Run 56 (730°C), and Run 58 (800°C).....	26
6-3 Nonhydrocarbon Gases in Simulated Run 55.....	27
6-4 Gaseous Hydrocarbons in Simulated Run 55.....	28
6-5 Gaseous Nonhydrocarbon in Simulated Run 56.....	29
6-6 Gaseous Hydrocarbons in Simulated Run 56.....	31
6-7 Nonhydrocarbon Gases for Simulated Run 58.....	32
6-8 Gaseous Hydrocarbons for Simulated Run 58.....	33

LIST OF TABLES

	<u>Page</u>
5-1 Thirteen Hydrocarbon Reactions Considered.....	21
5-2 Primary Biomass Vapor Reactions Considered.....	21

SECTION 1.0

INTRODUCTION

The heating of biomass in an oxygen-deficient situation is known as pyrolysis and has been used for centuries to produce charcoal, tars, wood alcohol, and other solvents. The traditional slow heating of biomass produces about equal amounts of gases, char, and tarry liquids. These tarry liquids have been promoted as boiler fuels, but they are not thought to be suitable for use in internal combustion (IC) engines. Current state-of-the-art dictates that the liquid fuels used for IC engines be either a hydrocarbon material, an alcohol, an ether, or mixtures of these.

Under certain very rapid pyrolysis conditions, valuable products can be recovered which are not predicted by chemical thermodynamic equilibrium. These nonequilibrium products can be varied considerably depending upon the reactor conditions selected. The products can contain large amounts of oxygenated oils or be almost entirely gaseous and contain a significant amount of very desirable unsaturated hydrocarbons such as ethylene and propylene. The chemistry of these unsaturated hydrocarbons is very well known and is the basis for a large part of the existing petrochemical industry. In the past, they have been used by the petroleum industry to make gasoline and by the petrochemical industry to make alcohols, plastics, etc.

Historically, the energy and chemical industries have used the most economical feedstock available, which was wood or cellulose until the fossil fuel age arrived. With the advent of cheap petroleum and natural gas, the industry became based on low-molecular-weight compounds, such as ethylene, for use as starting materials to make rubber, plastics, alcohols, and liquid fuels. Although the highest yields of ethylene may be made from ethane, the increase in cost and the decrease in availability of ethane gradually shifted the industry toward using less desirable feedstocks, even though the yields may be lower and the processing more difficult. The use of biomass as a source of ethylene and higher hydrocarbons via a rapid thermal reaction would have considerable merit, especially in areas without assured access to petroleum sources.

The conversion of biomass to ethylene and higher hydrocarbons via fast pyrolysis had been demonstrated by several isolated researchers at scales ranging from a few milligrams in batch experiments to continuous flow, bench-scale experimentation at nominal flow rates of 5 kg/h. In addition to the fundamental pyrolysis studies by Evans et al. [1], DOE's Biomass Energy Technology Division has sponsored a fast pyrolysis program at SERI having three areas of effort: laboratory-scale pyrolysis of a few milligrams of material from monolithic pieces of biomass to determine optimal heat transfer mechanisms; the bringing together of the several isolated fast pyrolysis researchers to compare methods, results, and conclusions as to the fast pyrolysis phenomenon [2]; and the ongoing investigation of fast pyrolysis of biomass with a continuous flow reactor to demonstrate the use of practical heat-transfer techniques and biomass feedstocks larger than fine powders.

SECTION 2.0

BACKGROUND

As was reported and demonstrated at the 11th Biomass Thermoconversion Contractors' Meeting [3], the laboratory-scale heat transfer experiments have shown that when biomass is moved relative to a red-hot Nichrome wire, the wire will cut through the biomass. The rate of cutting, or pyrolysis, can be as high as 3 cm/s when it is a very localized surface phenomenon. With this method of heat transfer, pyrolysis appears to proceed by the depolymerization, melting, and vaporization of the biomass without observable char formation; the term "ablative" seems to best describe this fast pyrolysis mechanism.

The rate of heat transfer from the red-hot metal surface to the biomass is extraordinarily high. Based on an estimated energy of pyrolysis of 2000 J/g, the 0.025-cm diameter wire moving across the biomass at 20 cm/s and penetrating at a rate of 3 cm/s was transferring 3500 W/cm^2 , which is very impressive compared to the mere 15 W/cm^2 radiated by a black body reactor wall at 1000°C . Thus, this solid convective approach to pyrolysis transfers energy to the biomass at rates over two orders of magnitude greater than black body radiation at similar wall temperatures. This would imply that a properly configured pyrolysis reactor achieving solid-convective heat transfer could have over 100 times the throughput of a similarly sized reactor relying only on radiative heat transfer. These inferences have been confirmed in recent work by Lede et al. [4] in which measured solid convective heat transfer coefficients into wood were 1-1/2 to 3 orders of magnitude greater than radiative heat transfer coefficients.

The mechanism of this solid-convective heat transfer appears to be the conduction of heat across a very thin film (thought to be about $10 \mu\text{m}$ thick) from a metal surface at perhaps 1000°C , while the biomass depolymerizes at about 475°C to primary tars which are wiped away and/or vaporized. Since heat conduction is proportional to this large temperature difference divided by the very small film thickness, very high heat fluxes are predicted. Because the surface regression rate is nearly the same as the thermal penetration rate, any biomass which is located more than a calculated $15 \mu\text{m}$ from the pyrolyzing surface is still at the low initial temperature and is unaffected by the ablative pyrolysis taking place. Consequently, this char-less, ablative pyrolysis will proceed in a similar manner whether the biomass is a 1-cm chip or a fine, $50\text{-}\mu\text{m}$ powder [5]. Because the pyrolysis front moves so quickly through the biomass, the temperature gradient is very steep with a calculated heating rate of about $500,000^\circ\text{C/s}$ [6].

The ability to use wood chips rather than a fine powder or dust as feedstock would improve the overall process with respect to an estimated 10% to 15% process energy reduction, less equipment to amortize, and enhanced safety by eliminating dust explosion hazards in storage bins, transfer lines, etc. The pyrolysis reactor concepts, which we are developing, involve a very high throughput reactor in which entrained biomass particles at high velocities enter tangentially into a cyclone or vortex tube as shown in Fig. 2-1. The vortex tube wall is externally heated so that pyrolysis takes place as the

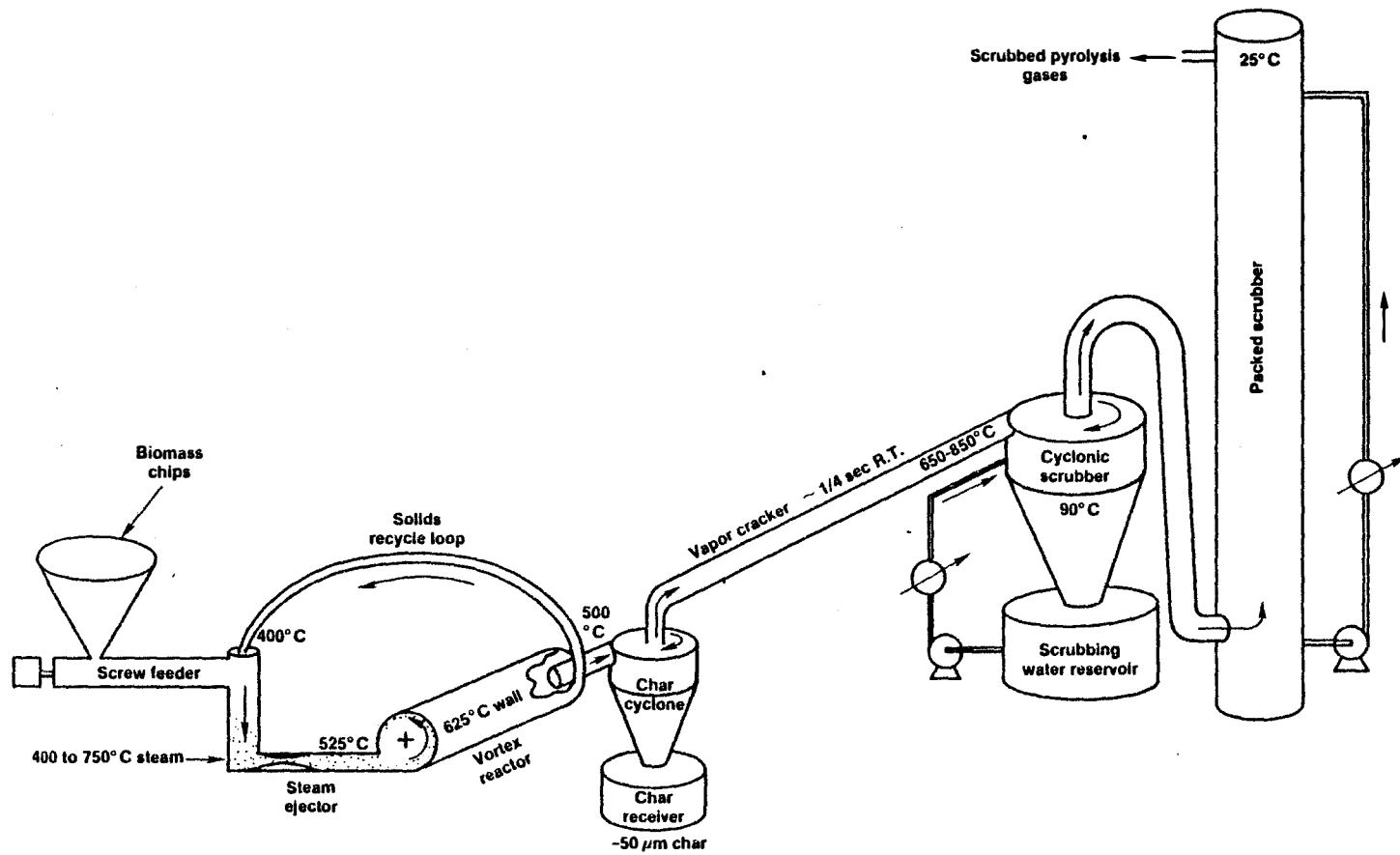


Figure 2-1. Schematic of Ablative Pyrolysis System

biomass slides and bounces along the inside surface. This contact and relative motion of the hot wall and the biomass particles, if intimate, is analogous to the hot-wire pyrolysis mentioned above. The vortex section of the reactor is followed by a char cyclone and then a long tubular vapor cracking section to maximize gas formation. Detailed descriptions of the experimental hardware are given in References 7 and 8.

The system is operational and due to reactor design modifications made in FY 1984, a significant improvement in operation has been achieved. The biomass throughput has been increased from about 12 kg/h with steam-to-biomass weight ratios (S/B) between 1.5 and 2.5 to a new record of 32 kg/h with an S/B of only 0.8. This high throughput has been accomplished by lowering the cyclone reactor wall temperature so that mostly biomass vaporization, with some char forming reactions, take place, but not high temperature gas cracking nor char gasification reactions. As shown in Fig. 2-1, a recycle loop was added to the cyclone reactor exit to return partially reacted feedstock to the reactor inlet. The char is also recycled around the cyclone reactor until it is ground to a fine powder and is then re-entrained with the product vapors and steam. These modifications provide for the separation of major pyrolysis steps so that they can be optimized for a system to produce olefins for subsequent conversion to transportation fuels or to produce primary oils for use as boiler fuels or subsequent upgrading.

The biomass vaporization takes place at about 475°C. By operating the cyclone reactor wall at 625°C, sufficiently rapid biomass vaporization takes place to result in an intermediate product containing 65% to 75% organic vapors, 5% to 10% gas, 10% char, and 10% to 15% water formed by the reaction. Although it is not normally done, these organic vapors could be condensed and recovered with high efficiency using wet scrubbing.

Mathematical modeling of cellulose pyrolysis has resulted in a six reaction model using kinetics reported by four different research groups using widely varying conditions. This model has been shown to be very predictive for low heating rates in a TGA analysis (40°C/min) and to be useful in gaining a better understanding of pyrolysis at higher heating rates [9].

Previous experimental results are given in detail in References 8, 9, 10, and 11. Work so far has demonstrated that substantial yields of olefins and BTX can be obtained from sawdust (as high as 15 and 10%, respectively, expressed as a percent of carbon in the wood). Key questions currently being addressed relate to optimized operating conditions for the cyclone reactor and the vapor cracker, the provision for higher heat transfer rates through the cyclone wall, and the development of a mathematical model to describe observed behavior and predict performance in the existing reactor and in scaled-up reactors in the future. In addition, the high yields of "primary" biomass vapors suggest that some form of catalytic upgrading to a gasoline product would be a significant achievement. The use of zeolite catalysis to achieve this conversion is currently being studied.

SECTION 3.0

VORTEX PYROLYSIS REACTOR

3.1 Pyrolysis System Modifications

The pyrolysis system, as it was installed in the new location at SERI's Field Test Laboratory Building, has been upgraded electrically. In the previous location, only 115 and 208 volt electricity was available. In the new location, we have 240 and 480 volt electrical power available, which effectively delivers 33% more power to the resistance heaters for the vortex reactor, the vapor cracker, and the steam superheater. This additional power will allow higher throughputs to be attained with the system. All of the power supplies for the heaters have been converted for use at the higher voltages.

One of the major thrusts for this fiscal year was to investigate the operation of the pyrolysis system at high biomass throughputs. For the vapor cracking kinetic study conducted last fiscal year, a biomass throughput of about 15 kg/h was selected because the recycle loop was effective in capturing the unreacted biomass particles at this flow rate. At higher flows the efficiency of the recycle loop decreased to unacceptable levels, although it remained functional and did not plug up. A study was made to determine what measures could be taken to increase the efficiency of the recycle loop. An examination of the inside of the vortex reactor revealed that as the particles left the middle section of the vortex reactor having the raised helical rib, they encountered a surface discontinuity which would tend to make them lift off of the surface. In addition, the last two inches of the reactor's ID were smooth and did not guide the particles to the recycle loop's entrance. To remedy this situation, a new aft-end section was fabricated from 316 SS, which extended the helical rib so as to guide the particles directly to the entrance of the recycle loop. In addition, the tangential direction of the recycle loop was changed from horizontal to vertical to reduce the length of the recycle loop and the amount of curvature needed to reach the feeder adapter. These modifications to the vortex reactor system were expected to aid the recycle of partially pyrolyzed biomass particles so that recycle efficiency would be retained at much higher throughputs than in the past.

After Run 65, the last three inches of the helical rib were ground off to allow the solids to more easily reach the recycle loop entrance. Cold flow tests with nitrogen as the carrier gas were then made, which revealed that even with the obstructive portion of the rib removed, the solids still accumulated in the "dead-zone." An insert was then made to extend the tangential entrance of the recycle loop from the 9 o'clock position back to the 6 o'clock position where the solids accumulated. This drastically shrank the "dead-zone" to result in only a very slender, 1/2-inch high crescent of particle accumulation extending from about 3 o'clock to 6 o'clock. This configuration was used for Run 64.

The char receiving drum was modified to allow the sampling of the char as it was being collected during a run. A stainless steel funnel was fabricated having a half-inch tube as the outlet. The tube had a 90° bend in it. The funnel was located underneath the char cyclone (inside the char receiver drum)

to catch the char. The half-inch tube penetrated the side of the char drum through a compression fitting and then made another 90° bend before passing through a ball valve. The compression fitting was tightened enough to form a seal at these low pressures, yet loose enough to allow the funnel assembly to rotate. In normal operation, the funnel is rotated upside down to keep it empty, and the valve is closed. To sample the char, the funnel is rotated 180° to catch the falling char, and the valve is opened. The char is quickly collected in a container fitted with glass wool. Adequate ventilation ensures that toxic concentrations of pyrolysis gas do not accumulate.

The design concept of the cyclone scrubber was to condense secondary tars with water sprays, rather than on a cool surface. This approach was chosen because the secondary tars have very poor flow characteristics and tend to plug heat exchanger tubes. However, the primary condensates we are now making at low pyrolysis severities have much better flow characteristics. The cyclone scrubber is being modified to allow it to be operated as a cyclonic condenser with surface cooling. In conventional heat exchangers, the heat transport normally exceeds mass transport of the condensates from the process stream to the heat transfer surface, which results in homogeneous condensation to form aerosols. We will determine if the centrifugal forces in the cyclone condenser can reverse this balance of heat and mass transport. If condensation occurs only in the boundary layer, the condensates will have a very short distance to go before being centrifuged onto the wall and collected. Aerosols that escape the cool boundary layer will have a tendency to reevaporate, as long as the bulk gas temperature is high. This concept requires vigorous cooling of the surfaces involved to maintain boundary layer temperatures below the dew point. The conversion of the cyclone scrubber to a cyclonic condenser with internal and external cooling was completed.

In addition to the conversion of the cyclone condenser, the upper portion of the packed scrubber was converted to an electrostatic precipitator. The "brush-pak"™ has been removed, leaving only the ceramic Burl saddles in the bottom 15 inches of the packed scrubber. The electrostatic precipitator section will consist of an electronically charged, small diameter wire suspended from the top of the scrubber, following common practice. The electric field created by the wire will charge the submicron aerosol smoke particles to cause them to migrate to and impinge on the cylindrical surface of the scrubber. These modifications should greatly enhance the ability to collect the primary oil condensates to better close our mass balance and to provide a more complete oil sample for analysis and upgrading. We will be testing the effectiveness of these modifications in the near future.

The cyclone scrubber was modified to allow the catalytic, slipstream reactor to pass through it into the vapor cracking section. It is planned to load this reactor with new catalyst from Mobil.

3.2 Pyrolysis Experimentation

The rebuilt ablative-pyrolysis system in the Field Test Laboratory completed a shakedown sequence to progressively identify and eliminate problem sources. The first attempt to operate the new system with feed was successful. The purpose of this run was to progressively increase the sawdust input until an upper limit was reached. Starting with a constant steam rate of 30 kg/h and a

sawdust feed rate of 12 kg/h, the sawdust feed rate was gradually increased to 35 kg/h. The recycle loop remained open during this entire run. After a short period of operation at this last throughput, the char drum became full so that the char cyclone was ineffective. This caused the char to accumulate downstream in the cyclone-scrubber-water filters, which led to plugged filters and a loss of scrubbing water. This experiment showed that with the existing vortex reactor configuration, as the sawdust throughput was increased to around 35 kg/h, partially reacted feed was able to escape the vortex reactor. This resulted in an abnormally high solids accumulation in the char receiver drum. The axial outlet of the vortex reactor needed to be modified so as to encourage the partially reacted feed particles to enter the recycle loop rather than the axial outlet. In addition, a char sampling technique needed to be developed to allow sampling of the char during the experiment.

A pyrolysis run was made to evaluate the new char sampling system and the reactor modification. The feed rate was started at 10 kg/h and increased in 5 kg/h increments. Between a feed rate of 20 and 25 kg/h, the nature of the char changed from a fine powder to a fine powder with larger particles mixed into it. The presence of larger particles in the char sample indicated that the char was leaving the vortex-reactor/recycle-loop system before pyrolysis was completed. The power demand indicated by the vortex-reactor heaters during this run implied that the system was operated at less than one-half of the potential throughput.

Since the program has an increased emphasis on the production of primary oil vapors for upgrading, a more direct measurement of these oil yields is being sought. The pyrolysis system had been modified to allow the gas scrubbing system to be operated to strip the volatiles out of the gas stream. In this scrubbing mode, the system was tested to verify that a mass balance could be made accurately. A quantity of water was carefully weighted and added to the scrubbing system and the pumps operated. The system was then drained and the water reweighed. Closure of the mass-balance was 99.9%, but only after the packed scrubber was allowed to drain overnight. This test indicated that holdup in the packed scrubber could result in poor closure of a mass balance, and time must be allowed for the rather slow drainage from the packing, even with a low viscosity material such as water.

The pyrolysis system was operated using house nitrogen (cryogenic source) as the carrier gas at a carrier-to-biomass ratio of 1.5. The goal of this operation was to obtain high oil yields and to more directly quantitate that yield than had been done in the past. The feed rate was a nominal 15 kg/h. In order to preserve the delicate primary vapors, the vortex reactor wall temperatures were set at 600°C. The vapor cracker was preheated to about 400°C and then was turned off for the duration of the run. The nitrogen temperature was originally set at 500°C, but later increased to 550°C in an attempt to increase the outlet product vapor stream temperature from 435° to the desired 475° to 500°C. No increase in the product vapor stream temperature was noted. In retrospect, it appears that the increased energy content of the carrier gas was converted to the latent heat of pyrolysis because there was a significant amount of unpyrolyzed material which escaped the vortex reactor. This scorched material was retained by the char cyclone until it became filled, at which point the solids were entrained into the scrubbing system. The presence of absorptive solids in the scrubbing system made it

impossible to quantitate the oil and water yields as had been planned. Although similar temperatures had been successfully used in Run 40, a reexamination of the Run 40 data revealed that the feed rate used was only about 6 kg/h. The use of the low temperatures did serve to avoid the cracking of the primary oil vapors produced, but the feed was only partially pyrolyzed as it passed through the reactor. GC analysis of the vapor stream before and after passing through the vapor cracker revealed virtually no change in the percentage of carbon dioxide, which is a sensitive marker for vapor cracking. A further comparison to previous data when the system was operated to produce little vapor cracking in the vortex reactor revealed that higher carrier gas temperatures of 750°C had been used to achieve the apparently necessary higher product vapor exit temperatures of about 500°C for exhaustive pyrolysis of the feed.

Pyrolysis Run 65 was planned to quantitate the yields of primary oils by direct measurement of the collected condensates. However, at the beginning of the run, it was observed that there was an accumulation of large char particles at the aft end of the vortex reactor. This area appeared to be an aerodynamically "dead-zone." The effect of this solids accumulation was to provide a ramp for the premature axial escape of partially pyrolyzed particles from the reactor to the char cyclone. This effect has apparently contributed greatly to the recent lack of exhaustive pyrolysis of the feed particles and, consequently, to the overloading of the char removal system experienced on the last several runs. As viewed through the quartz window near the entrance of the vortex reactor, the tangential recycle loop entrance location had been relocated from the 6 o'clock to the 9 o'clock tangential position when the helical rib was extended to guide the solids directly into the recycle loop entrance. The helical rib continued past the recycle loop entrance to end at the aft bulkhead at about the 7 o'clock position. The very end of the spiral rib then acted as a dam to begin the solids accumulation. The run was interrupted to remove the cantilevered insert from the axial outlet, but this only allowed the particles an easier path to the axial outlet and did not activate the aerodynamically "dead-zone" to remove the solids accumulation. No mass balances were attempted on this run.

Run 66 was made with nitrogen as the carrier gas and at a nominal feed rate of 7.5 kg/h to try to obtain a direct measurement of the oil production. Preliminary results indicate that the vortex reactor worked very well, as the char recovered was a very fine powder with no evidence of unpyrolyzed particles escaping prematurely. The char yield was only 9% by weight of the feed, also indicative of good, thorough pyrolysis action in the vortex reactor. Analysis of the aqueous condensates determined the amount of organics recovered as a percentage of the condensate.

Run 66 was made using dry nitrogen as the carrier gas to demonstrate the oxygenated oil yields by collection. Previously, the oil yields had been shown by difference to be about 70% by weight. Further analysis of the Run 66 data revealed the following amounts of recovered products: 9% char, 36.4% tars and oils, 17% gases, and 38% lack of closure. With an estimated 12% water of pyrolysis, about 26% organics were not recovered by the system. It is suspected that some of the volatile organics and scrubbing water were lost as vapors, but that most of the loss was as a misty, smokey aerosol. This aerosol would have had a loading of 91 gm/m³ of exit gas. Better mass

closure (84%) had been previously obtained in Run 42 in which steam was used as the carrier gas; however, the large amounts of scrubbing water and condensed steam in the calculations made the results subject to errors.

3.3 Summary of Vortex Reactor Effort

The current vortex reactor system has a heating capability which is not being fully utilized due to bottlenecks in the recycle loop. The ability to sample the collected char was added so that the effect of several different feed rates on char quality could be evaluated in one experimental run. Good char particle size classification was retained up to between 20 and 25 kg feed per hour. The raised helical guide rib was modified to guide the solids to be recycled into the entrance of the recycle loop. The location of the recycle loop entrance was changed from the 9 o'clock to the 6 o'clock position to aid the entrainment of heavy particles. However, due to increased interest in quantifying the oil yields, the upper limit of biomass throughput was not determined for the current vortex reactor configuration.

Experimentation to quantify the pyrolysis oil yields led to the conclusion that the use of large amounts of water for spraying in the cyclone scrubber and irrigation of the packed tower led to experimental errors that could best be resolved by eliminating the water. The lack of closure of the mass balance is attributed to volatiles (including water) being stripped off by the pyrolysis gas stream and to aerosols forming, both of which are not recovered from the pyrolysis gases by the existing system. Modifications to the system to improve the oil recovery are in progress.

SECTION 4.0

ZEOLITE CATALYST EVALUATION

4.1 Introduction

In the last annual report [12], a review was made of zeolite catalysts. It was speculated that Mobil's ZSM-5 zeolite catalyst appeared to have the potential to convert the low-molecular-weight primary pyrolysis oil vapors to a high-octane gasoline product. The outstanding feature of such a process is that it could use the primary vapors as a feedstock without the need for hydrogen or complicating steps such as vapor compression or vapor condensation-pumping-evaporation needed for high-pressure hydrogenation processes. After removal of the char in a hot cyclone, the primary pyrolysis vapors would be passed through the catalyst bed held at 2 to 3 psig and about 400°C. The molecular weight of the primary vapors is thought to be minimized immediately after their formation, before bimolecular reactions start to create higher-molecular-weight aromatic secondary tars. Since the zeolite catalysts act as molecular sieves, large and bulky molecules cannot enter into the catalytically active interior of the catalyst. Molecules more bulky than xylene have a very difficult time diffusing through the medium pore size ZSM-5, although less bulky molecules such as n-butyl formate and furfural alcohol diffuse quite readily [13-15]. Consequently, it is thought that the pyrolysis vapors would be most reactive to the zeolite catalyst immediately after their formation, in a catalytic reforming reactor close-coupled to the pyrolysis system.

In order to make a quick, qualitative assessment of the effect of the catalyst on the full complement of organic, primary vapors, tests were run using the batch-pyrolysis, direct sampling, molecular-beam system used in the fundamentals pyrolysis task by Evans at SERI.

4.2 Experimental**4.2.1 Catalyst**

Approximately 10 grams of pure, ammoniated ZSM-5 were donated to the program by Mobil Research and Development Corporation to be used in our initial experimentation. This material appeared to be a very fine, crystalline material having a typical diameter estimated to be 5 to 10 μm by microscopic comparison to 4 to 8 μm diameter quartz wool fibers. In order to minimize the rate of coke formation on the catalyst [15], we diluted the catalyst with 10 parts by weight of quartz wool per part of catalyst. Microscopic examination of the catalyst-loaded wool indicated that the catalyst appeared to have a mild attraction (possibly electrostatic) to the wool which could survive initial temperature cycling in hot helium.

4.2.2 Reactors

The catalytic reactor for the first series of experiments, MOD A, consisted of a 25-mm quartz tube that was 25 cm long. This tube was placed on top of another quartz tube, which served to preheat the carrier gas. The reactor

tube was loosely packed with 0.3 g catalyst on quartz wool. The sample holder was located near the top of the preheater tube. The preheater tube and the catalytic reactor tube were heated independently by two separate furnaces. The furnace for the preheater was controlled by a thermocouple in the vicinity of the sample holder. The furnace for the catalytic reactor was controlled by a thermocouple located inside the reactor about two inches from the outlet; this furnace was to maintain the temperature attained by the carrier gas in the preheater. Experimentation with methanol vapors showed that the catalyst was very reactive, as had been reported (14). The high reactivity suggested that the measured temperature was considerably lower than the true gas temperature, due to end effects of the upper tube furnace where the thermocouple was located.

The reactor for the second series, MOD B, was very similar to that previously used, but a 304 SS tube was used for the catalytic reactor. To minimize radiation errors, the controlling thermocouple for the catalytic reactor was inside the stainless steel reactor vessel about 3 inches from the exit. A new catalyst/quartz wool mixture was used. The thermocouple controlling the preheater was placed at the outlet of the preheater (between the two furnaces) and inside a half-inch diameter stainless steel tube through which the hot gases passed.

For the third and last test series, a 20-mm diameter, single-piece, quartz, preheater-catalyst reactor was used (MOD C). The sample holder was located in a similar location as before. In order to have a more isothermal catalytic reactor during the pulse of organic vapors, a heat-sink was added between the sample holder and the catalyst bed. The heat-sink consisted of about 26 grams of 0.020-inch Nichrome wire cut into ~1 cm lengths and was calculated to be sufficient to maintain isothermal conditions to within 10°C during the pulse of vapors. The controlling thermocouple for the catalytic reactor was placed about three inches into the catalyst/quartz wool mixture to try to avoid end effects. Stainless steel shim stock was wrapped around the quartz reactor to minimize radiation from the furnace wall to the thermocouple through the quartz wall. Due to the smaller diameter of this reactor, the gaseous residence times were about half that of the other reactors. The measured temperatures in this reactor are thought to be the most accurate of the three reactor designs.

Although the location and shielding of the thermocouples underwent considerable change to improve the accuracy of the gas temperature measurement, it is thought that the measured temperatures were not necessarily representative of the true gas temperatures. The measured temperatures within a test series are relative to each other, but are not thought to be accurate temperature measurements due to radiation induced errors. This uncertainty is not important for these early screening experiments.

The effluent from the catalytic reactor was passed directly into SERI's molecular-beam mass spectrometer (MB-MS) for real-time analysis in all tests. This apparatus is described in Ref. 1. Sample sizes used were typically 0.090 g for liquids or 0.030 g for solids. Helium at 2 liters/min was used as the carrier gas, which resulted in gaseous residence times of one to two seconds depending upon the catalytic reactor. The duration of each vapor pulse varied between about 20 seconds for the methanol and 40 seconds for the powdered solids.

4.2.3 Experiments

To verify the inertness of the reactor system without catalyst, blank runs were made with methanol vapors, cellulose (PH-102 Avicell) pyrolysis, and furan [as shown in Fig. 4-1 (bottom) and Fig. 4-4, respectively]. The quartz wool was judged to be noncatalytic.

With the ZSM-5 loaded wool, the conversion of methanol to dimethyl ether (m/z 45⁺, 46⁺) was very clearly observed with the MB-MS as seen in Fig. 4-1 (middle). The appearance of low-molecular-weight hydrocarbons also occurred at the more severe temperature conditions employed, as seen in Fig. 4-1 (top). The behavior of methanol in the zeolite reactor appeared to qualitatively conform to that reported by Mobil personnel in the literature [14], except that xylene appeared before benzene (perhaps by butadiene homopolymerization reactions followed by aromatization to produce xylene). Major peaks were observed for mass numbers corresponding to ethylene, propylene, butene, pentene, and hexene, as well as for xylene.

Cellulose vapors were seen to be very rapidly converted to a new product slate by the ZSM-5 catalyst, as seen in Fig. 4-2 (top). Most of the peaks in the new product slate were similar to those seen in the more severe methanol runs with the exception of two new peaks at 68 and at 82 m/z . The identity of these two peaks has not been firmly established; i.e., the m/z of 68 could be cyclopentene and/or furan and the m/z of 82 could be cyclohexene and/or methyl furan. However, as shown in Fig. 4-3, using furan vapors as feedstock suggested that furan may be at least as refractory as dimethyl ether to the ZSM-5 and that furan may well be a by-product of zeolite catalysis of cellulose vapor decomposition.

The primary pyrolysis of cellulose is affected by the presence of acid catalysis with the enhanced formation of furfural, as well as other products such as levoglucosenone [16, 17]. The formation of furan and alkyl furans may be due to the acid-catalyzed dehydration of the cellulosic primary vapor products by the zeolite acid sites. The aromatic stability of furan may prevent the removal of the last oxygen from the original carbohydrate structure by the catalyst.

A screening test with milled sweet-gum lignin and a lignin model compound (vanillin) in the MB-MS showed that these pyrolysis vapors were apparently too bulky to easily enter the pores of the ZSM-5 catalyst, as had been observed by Chantal with supercritically extracted poplar oils [18]. The compounds detected at the exit of the catalyst bed were those expected due to thermal reactions. A test with -80 mesh pine flour suggested that these biomass vapors react with the catalyst independently of each other; the lignin-derived vapors that passed through the catalyst bed were essentially due to thermal effects as a result of the temperature and residence time used, whereas the carbohydrate-derived vapors were converted rapidly by the catalyst. The primary pyrolysis spectrum of -80 mesh pine is shown in the bottom of Fig. 4-4. This spectrum is typical of the primary pyrolysis of softwoods with major peaks derived from cellulose (m/z 's 162, 144, 126, 98, 85, 73, 60, 57, 43, 32), hemicellulose (m/z 's 114, 96, 60), and lignin (m/z 's 180, 176, 164, 152, 150, 138, 124, 110). The effect of zeolites on the wood vapors is shown in the spectrum at the top of Fig. 4-4. The cellulosic primary peaks have

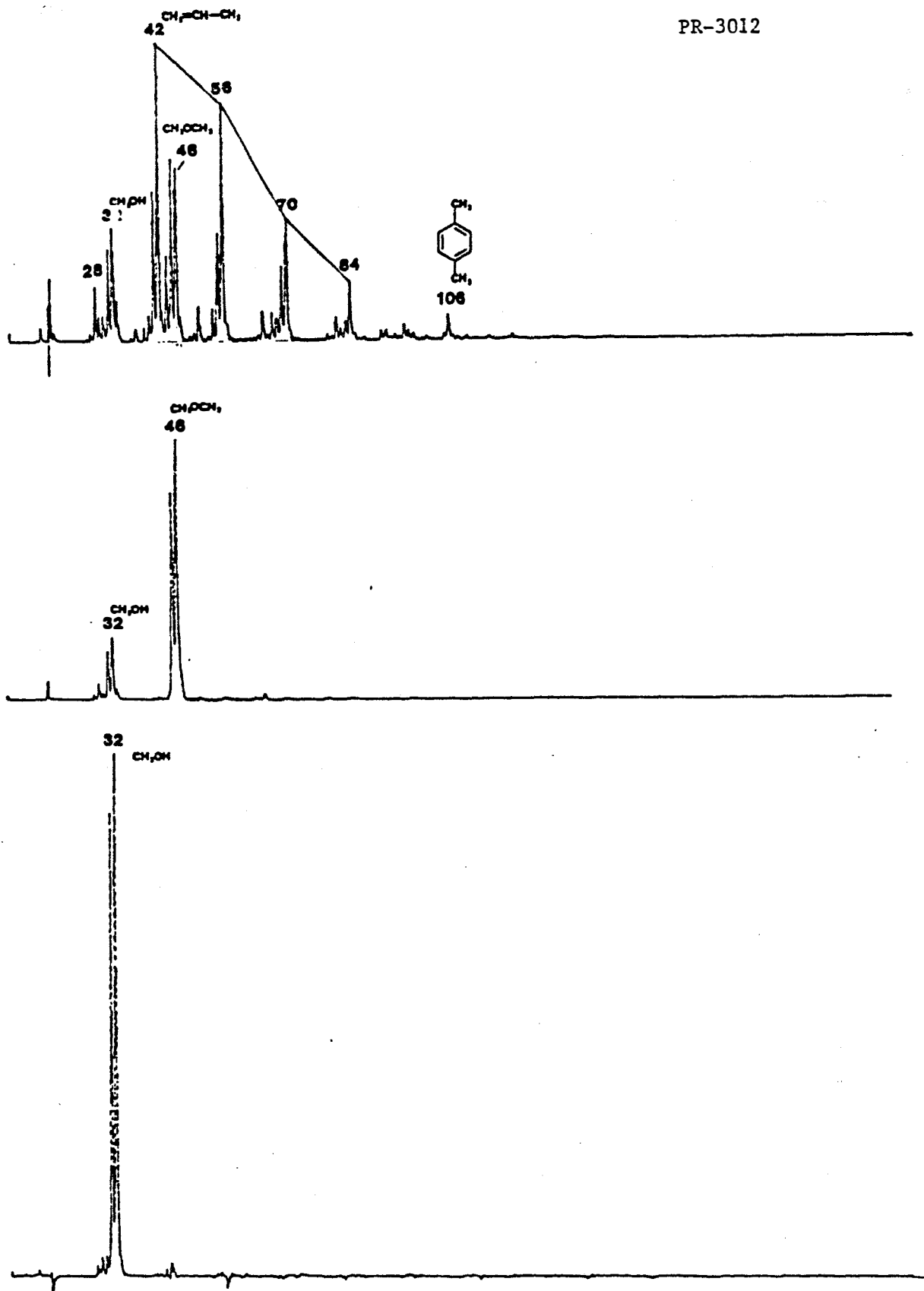


Figure 4-1. Mass Spectra Showing the Effect of Zeolite Catalysis on Methanol. Bottom, MeOH over quartz wool with no catalysis (MOD C reactor); middle, low severity zeolite catalysis to dimethyl ether (MOD C reactor); top, moderate severity conversion to hydrocarbon products (MOD B reactor).

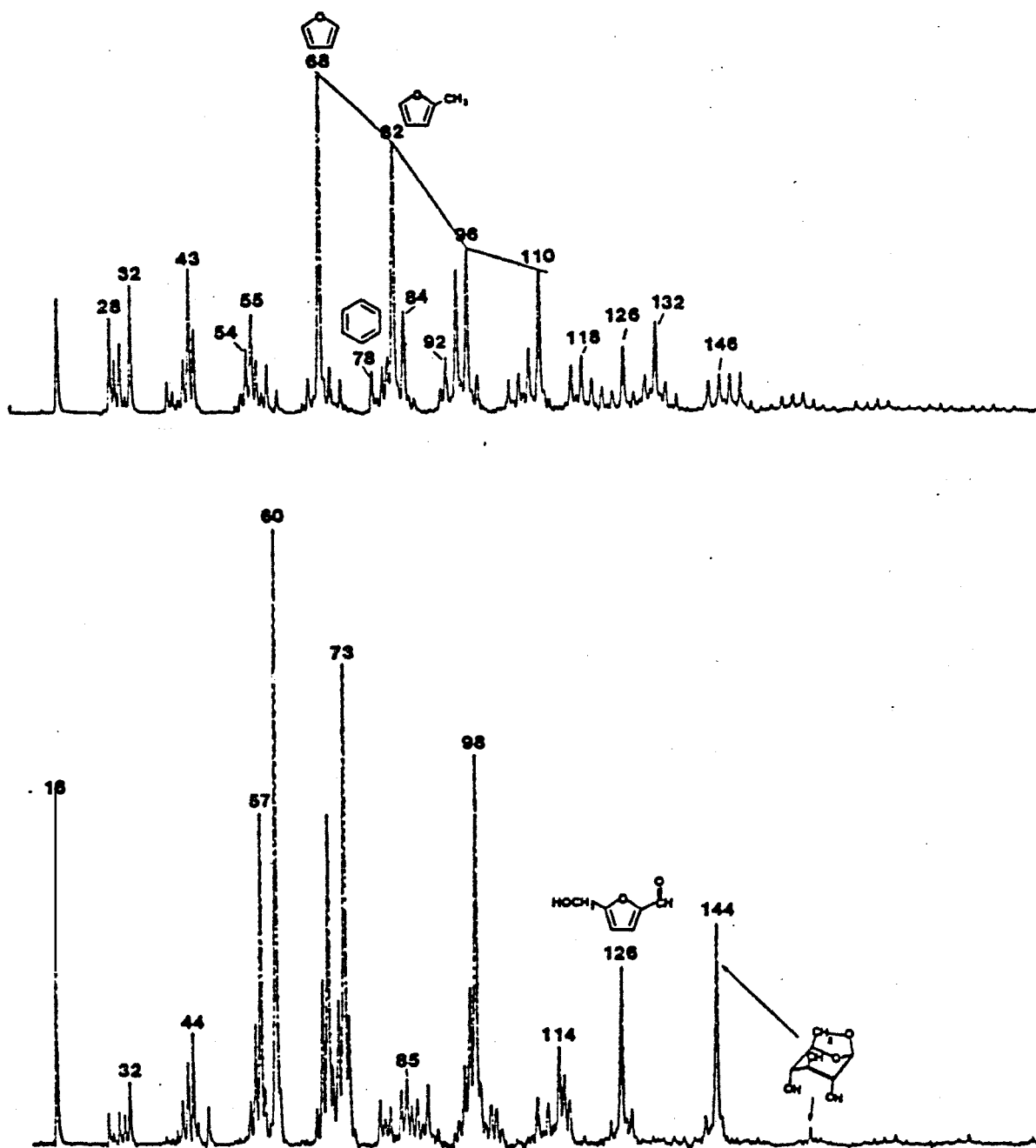


Figure 4-2. Mass Spectra of the Effect of Zeolite Catalyst on Cellulose-Derived Vapors. Bottom, vapors over quartz wool blank showing preservation of the primary species; top, products slate from zeolite conversion showing nearly complete conversion to deoxygenated and other new products (MOD C reactor).

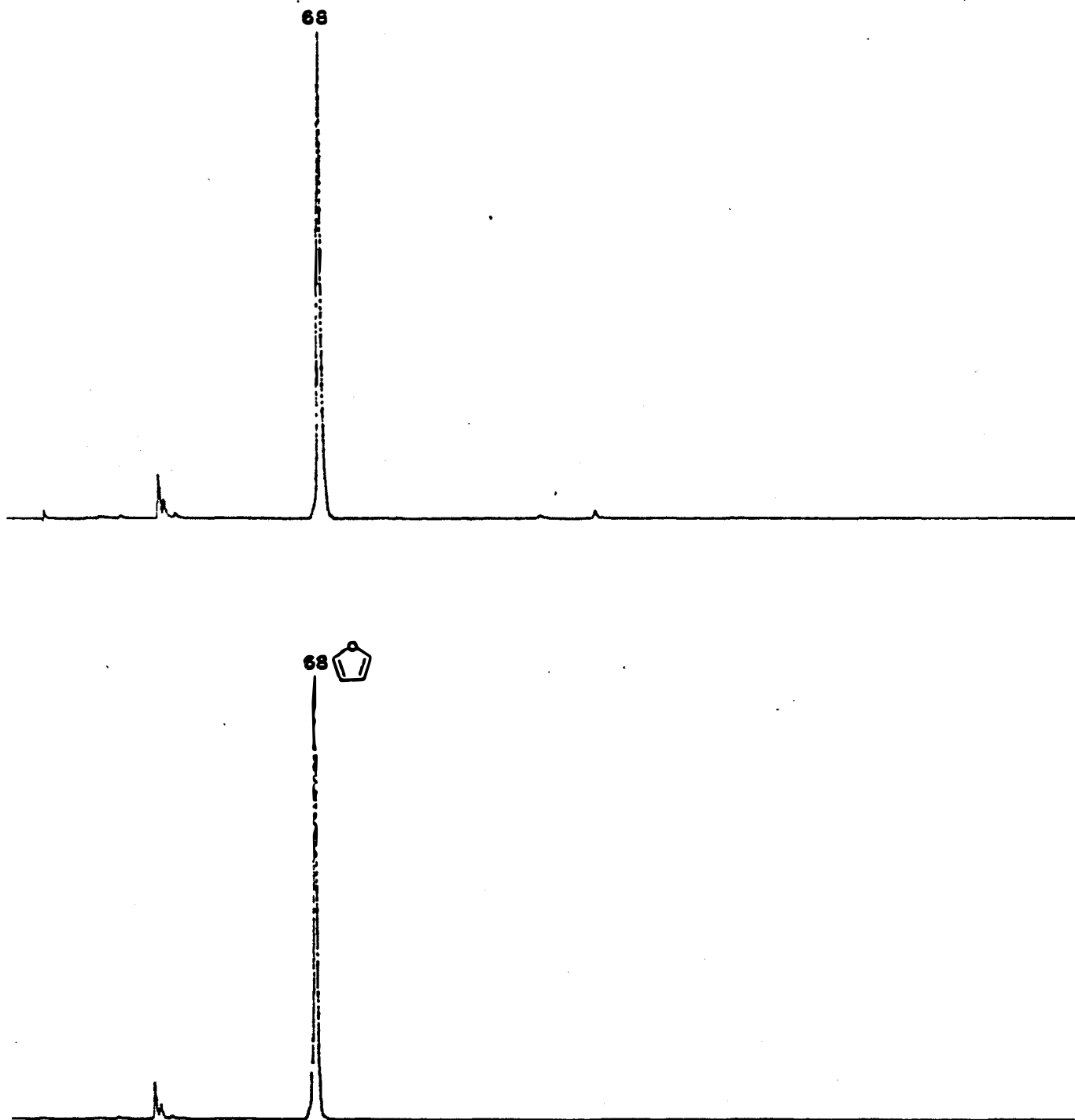


Figure 4-3. Mass Spectra of Furan over Quartz Wool Blank (bottom) and Zeolite Catalyst (top) Showing No Major Conversion under Conditions Used in These Experiments.

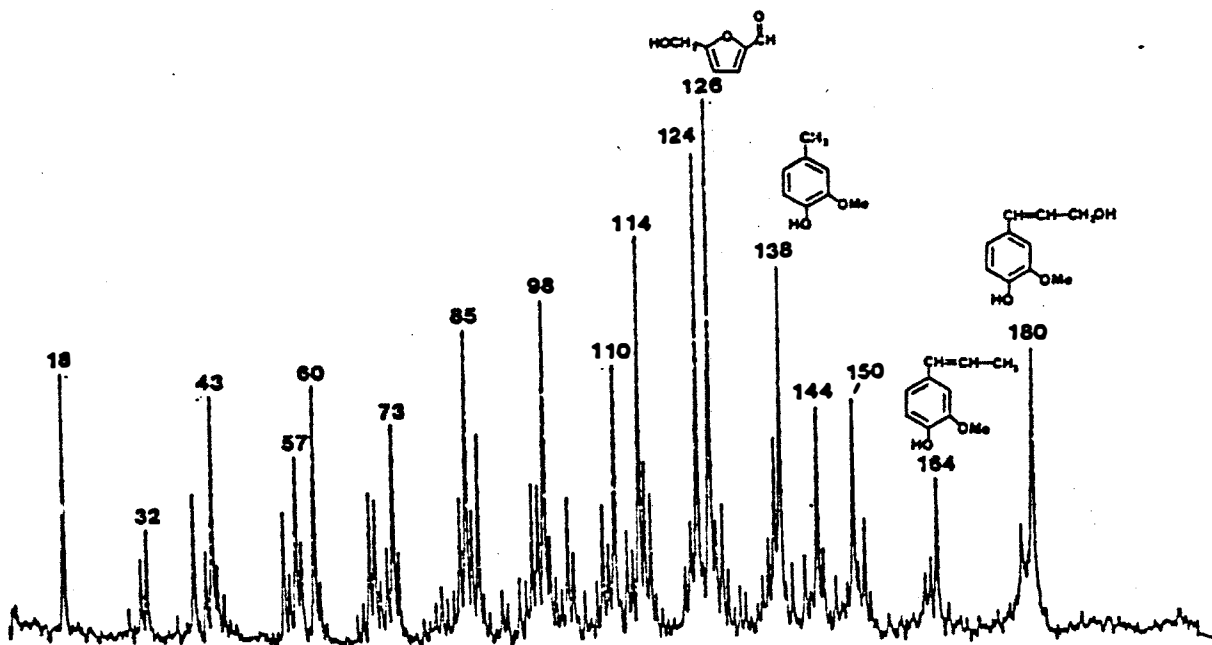
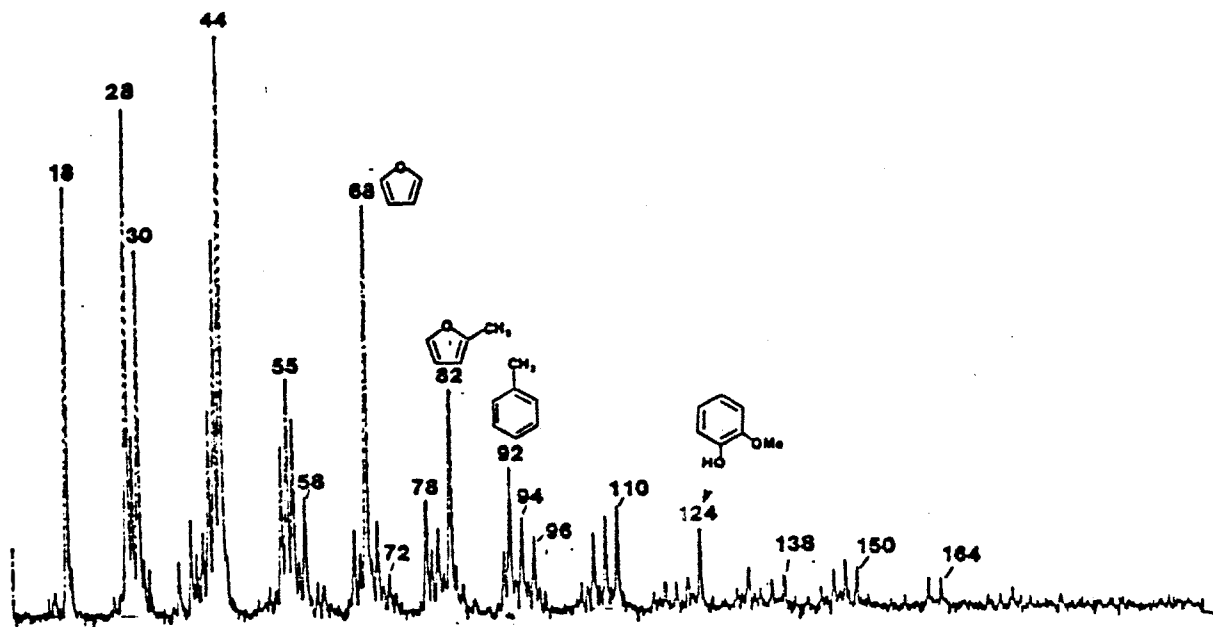


Figure 4-4. Mass Spectra of the Primary Pyrolysis of Pine Wood (Bottom) (obtained in 900°C steam/helium and 5-20 ms residence time) and the Product Distribution After Zeolite Conversion (top). The experiment shown at the bottom was not passed over quartz wool and is not a blank, but rather a reference for the zeolite and thermal effects. See text for discussion (MOD B reactor).

been completely removed and give the product distribution observed for pure cellulose. The heavier major lignin peaks (m/z 180 and 178) have been removed completely, but past experience has shown these peaks to be removed by thermal cracking at these temperatures and residence times. The more stable species guaiacol (m/z 124), methyl guaiacol (138), vinyl guaiacol (m/z 150), and isoeugenol (m/z 164) may survive unaltered by either the catalytic or thermal treatment. The amount of lignin material that forms coke on the catalyst is not known. These first tests did not quantitate the amount of coking on the catalyst, which will be of major concern in future, detailed catalyst studies.

4.3 Projected Product Quality Considerations

The presence of furans in the gasoline product has not been proven but is very probable. Although the furans are oxygenated, they are nonpolar and, consequently, insoluble in water and soluble in aromatic hydrocarbons. They have good thermal stability and motor blending octane numbers (BMONs). The BMON of furan is between 125 and 175 [19]; that of methyl furan is 92 [20]; and that of dimethyl furan is between 150 and 200 [21], depending upon the nature of the blending stock. The high cost of furan at about \$7.50 per gallon had apparently precluded serious thought of using it as a gasoline octane improver. The furans would most likely be left in the gasoline product.

The phenols and other lignin-derived fragments may need to be removed, e.g., by distillation or with a caustic wash to avoid corrosion problems, but they are reported to have excellent blending octane values. For example, p-cresol has BMON of 158 in a 78 octane base stock [20]. Guaiacol has a reported research blending octane number of 129 [22]. The caustic-extracted phenols could be reacted with dimethyl sulfate to form the methyl-phenyl ether and then added back to the gasoline product [23, 24]. There will need to be extensive characterization studies of the gasoline product when it is available in gallon quantities.

4.4 Maximum Yield Projection

Lignin-derived vapors do not seem to be affected greatly by the molecular sieve ZSM-5 catalyst, so that conversion of biomass to gasoline is projected to be essentially a conversion of the carbohydrate fraction of the biomass. The exothermic heat of reaction of the carbohydrate-derived vapors to form naphthenic gasoline was calculated to be about half of the heat released per unit weight of gasoline when made from methanol. The stoichiometry of converting cellulose to gasoline (toluene), water, and carbon dioxide suggests a maximum yield of 0.38 lb of gasoline per lb of cellulose vapor. Assuming a 70 wt % yield of biomass vapors containing 75 wt % carbohydrate vapors, a maximum gasoline yield of 55 gallons per ton of feed was calculated. At \$30 per dry ton of feedstock, the feedstock cost would be at least \$0.55 per gallon of gasoline. This simple process would result in a thermal efficiency of 43%. (For comparison, a crude oil, which might produce 80% by volume gasoline, would have a feedstock cost of \$0.89 per gallon of gasoline at a feedstock cost of \$30 per barrel.) If the lignin in the biomass were to preferentially form the char, the vapors would be more cellulosic and be more reactive so that yields of up to a maximum of 73 gallons gasoline per ton of biomass would be theoretically possible, with a thermal efficiency of 57%.

4.5 Cooperative Agreement with Mobil

We have made a modest cooperative agreement with Mobil Research and Development Corporation in which Mobil will supply catalyst expertise and pound quantities of proprietary catalysts formulated for use with biomass vapors. We will conduct experimentation using the biomass vapors from our pyrolysis system in a fixed-bed, ZSM-5 filled, catalyst reactor. The pyrolysis system would be close-coupled to the catalyst reactor to minimize thermal degradation of the very reactive primary vapors. Parameters we propose to investigate at this time are hydrocarbon yields, coking of the catalyst, regeneration of coked catalyst, and chemical species present in the expected hydrocarbon and oxygenated, aqueous liquid product phases. For a modest investment on Mobil's part, the probability of success for this process will be significantly enhanced. This could pave the way for a very significant future use of Mobil's ZSM-5 catalyst to convert primary pyrolysis oil vapors (derived from biomass) to high-octane gasoline, not only in the U.S., but also in many foreign countries that have both an abundance of biomass and a lack of petroleum resources.

4.6 Zeolite Evaluation Summary

Our conclusion at this point in the investigation is that the MB-MS clearly shows that the oxygenated vapors derived from the fast-pyrolysis of carbohydrates are very reactive with ZSM-5 catalyst. A primarily hydrocarbon slate is formed, which appears to be rather similar in nature to that obtained when using methanol as a feedstock. This observation was not unexpected, based on extrapolating the previous findings of many others. The exciting aspect of this preliminary screening is that we feel our approach to biomass pyrolysis will produce a feedstock vapor for the ZSM-5 catalyst at a fraction of the cost of methanol due to the simplicity of the pyrolysis process.

We envision an atmospheric-pressure process involving only one temperature cycle, in which the biomass particles are vaporized at $\sim 450^{\circ}\text{C}$, the char removed in a hot cyclone, and the oxygenated vapors immediately passed through a bed of ZSM-5 catalyst to form gasoline, water, carbon dioxide, and a lignin-derived oil. The lignin-derived oil may be a candidate for subsequent hydrogenation due to its expected low oxygen content, or it may be used for process energy. We currently have the largest known fast pyrolysis system which has demonstrated the capability to produce the primary biomass vapors in a continuous fashion in the high yields of interest without the concurrent production of secondary, polycyclic-aromatic tars. (A much larger, 15 TPD biomass pyrolysis system is currently being developed by a private corporation, based on many of our concepts.)

Although the economic feasibility of this catalytic process will be heavily dependent upon catalyst life, these initial results are very encouraging with respect to the conversion of cellulose to hydrocarbons with a simple process operating at atmospheric pressure with modest temperatures and overall residence times of only a few seconds.

SECTION 5.0

COMPUTER MODELING OF BIOMASS VAPOR AND HYDROCARBON
CRACKING IN A TUBULAR REACTOR

The goals of this modeling were to increase the understanding of the oxygenated vapor cracking phenomena, to identify fruitful areas for research where current knowledge is incomplete, and to provide a tool useful for rapid parametric "experimentation" to evaluate new approaches to pyrolysis and/or scale-up.

In general, the philosophy of the model was to utilize "rule-of-thumb" assumptions as little as possible and to rely as much as possible on mechanistic descriptions of the physical phenomena. However, simple empirical relationships were used when the mechanistic approaches become unwieldy for an apparently marginal increase in accuracy. The entire program utilized less than 64 K bytes including the data bank, which allows its implementation with inexpensive desk-top computers rather than requiring a "mainframe" computer.

This program was written in enhanced basic for the Hewlett-Packard 9845A desk-top computer having 64 K bytes of RAM. The program prompts a series of inputs from the user such as: reactor diameter, reactor length, inlet pressure, steam-to-biomass weight ratio, entering process stream temperature, biomass feed rate, molar composition of gases entering the reactor, time step increment, time span of interest, and the reactor wall temperature in each of the six furnace zones. The user is then given a chance to correct any previous entries before computation begins.

The program then prints a paragraph summarizing the run conditions and prints out in columnar form the distance down the reactor, time, gas temperature; the amounts of remaining primary vapor, the secondary tar formed, and seven gaseous products.

Then the program enters the fourth-order Runge-Kutta loop and calculates the parameters needed to evaluate the 15 kinetic equations. The more involved fourth-order Runge-Kutta approach is used rather than the simpler Euler first-order method so as to attain a higher degree of accuracy in the numerical integration without resorting to much smaller time increments [25]. Mole fractions are converted to moles per volume (concentration) at the temperature and pressure existing at that location in the reactor.

The gas velocity is calculated and used to evaluate the Reynold's number, Fanning friction coefficient, and incremental length. The gaseous viscosity of each component is calculated based upon correcting the viscosity value at 750°C by

$$\mu_{T,i} = \mu_{750} \left(\frac{T}{750 + 273} \right)^{N_i} ,$$

where μ is viscosity and N_i is an exponential coefficient for species i [26]. The gaseous viscosities of the primary vapors, secondary vapors, and ethyl benzene were assumed to be the same as for toluene. The average viscosity of the gas mixture was calculated by

$$\mu_{ave} = \frac{\sum (\mu_i mf_i \sqrt{mw_i})}{\sum (mf_i \sqrt{mw_i})},$$

where mf_i is the mole fraction and mw_i is the molecular weight of species i [27].

The gaseous enthalpies of the 19 compounds considered are calculated with the use of empirical four-term polynomial heat-capacity equations for each component. These heat capacity equations are reported to have, in general, an average error of less than 1/2% and maximum errors of less than 1% [28]. The heat capacity of acrylic acid was used for that of the primary vapors and the heat capacity of anthracene was used for secondary tar vapors [29]. The heat capacity of the mixture is calculated by summing the product of the molar heat capacity of each component (C_{p_i}) and its mole fraction. The Prandtl number (Pr) of each component is calculated by the Eucken relationship

$$Pr_i = \frac{C_{p_i}}{C_{p_i} + \frac{5}{4} R},$$

where R is the ideal gas constant [30]. The thermal conductivity of each component (k_i) is calculated from a rearrangement of the definition of the Prandtl number

$$k_i = \frac{C_{p_i} \mu_i}{Pr_i}.$$

The average thermal conductivity of the mixture is calculated [31] by

$$k_f = \frac{\sum (k_i mf_i (mw_i)^{1/3})}{\sum (mf_i (mw_i)^{1/3})}.$$

The average Prandtl number for the gas mixture is then calculated based upon the average values of heat capacity, viscosity, molecular weight, and thermal conductivity of the gas mixture. The Reynolds number is also calculated based on the average properties of the gas mixture. The Fanning friction factor (F_f) is calculated based on an empirical equation for use with turbulent flow [32]

$$F_f = 0.00140 + 0.125 (Re)^{-0.32}$$

This friction factor is used to calculate the pressure drop incurred during the time increment.

The convective heat transfer coefficient is calculated by

$$h_c = \frac{0.023 k_f (Re)^{0.8} (Pr)^{0.33}}{D}$$

where D is the tubular reactor diameter and the Reynold's number is assumed to be greater 10,000 [33]. (If the Reynold's number is not greater than 10,000, a warning to the user is printed at the end of the program that the heat transfer coefficient is not entirely valid.) The convective heat transfer is then calculated.

The thirteen hydrocarbon reactions considered are shown in Table 5-1. The two competing reactions for the disappearance of the primary biomass vapors are shown in Table 5-2. The necessary three equilibrium constants and the fifteen reaction rates are calculated using the temperature and concentrations at the

Table 5-1. Thirteen Hydrocarbon Reactions Considered [34, 35]

$C_2H_6 \rightarrow C_2H_4 + H_2$	Ethane
$C_2H_6 \rightarrow 1/2 C_3H_8 + 1/2 CH_4$	
$C_2H_6 + C_3H_6 \rightarrow 1-C_4H_8 + CH_4$	
$C_2H_4 \rightarrow C_2H_2 + H_2$	Ethylene
$C_2H_4 + C_2H_2 \rightarrow C_4H_6$	
$C_2H_4 + C_2H_6 \rightarrow C_3H_6 + CH_4$	
$C_2H_4 + C_3H_8 \rightarrow C_2H_6 + C_3H_6$	
$C_3H_8 \rightarrow C_3H_6 + H_2$	Propane
$C_3H_8 \rightarrow C_2H_4 + CH_4$	
$C_3H_6 \rightarrow C_2H_2 + CH_4$	Propylene
$C_3H_6 \rightarrow 3/2 C_2H_4$	
$C_3H_6 \rightarrow 1/4 C_6 + 3/2 CH_4$	
$1-C_4H_8 \rightarrow 1/2 C_8H_{10} + 3/2 H_2$	Butene

Table 5-2. Primary Biomass Vapor Reactions Considered [12]

Primary vapor \rightarrow 0.637 Secondary tar + 1.27 CO ₂ + 3.96 H ₂ O
Primary vapor \rightarrow 1.383 H ₂ + 1.599 CH ₄ + 0.053 C ₂ H ₂ + 0.692 C ₂ H ₄ + 0.138 C ₂ H ₆ + 0.231 C ₃ H ₆ + 0.123 C ₄ H ₈ + 0.15 C ₆ H ₆ + 0.015 C ₇ H ₈ + 7.841 CO + 0.748 CO ₂

beginning of the time increment for use in the kinetic expressions. These reactions, rates, and equilibrium constants for the hydrocarbon reactions were taken with minor modifications from the petrochemical literature [34, 35]. Although free-radical reactions apparently would give a higher degree of accuracy of prediction, the 200 or so chemical reactions needed for a free-radical model are reported to result in a "stiff" system of differential equations requiring very short time steps which results in very long computational times [36, 37]. The thirteen hydrocarbon reactions chosen reflect the mechanistic outcome, but are summations of free-radical reactions. The reactions shown in Table 5-2 are those which were found in the derivation of the kinetic rate expressions for the primary vapor decomposition in the last annual report [12]. Note that the product slate for vapor cracking assumes that no water is formed during this reaction, which is based upon the close match-up of the elemental composition of the primary vapors to that of the dry secondary gases. It is assumed that these product slates from biomass vapors are independent of temperature, although the final products are affected by subsequent hydrocarbon reactions. The primary vapor is produced in the vortex reactor upstream of the modeled vapor cracker. The amount of primary vapor entering the reactor is calculated from the carbon dioxide content of the incoming gases, using the relationships established in Ref. 12. The primary oil vapor is highly oxygenated and water soluble, whereas the secondary tar is only slightly oxygenated and is not water soluble.

The moles converted by each reaction are then computed and used to calculate the change in each component species. Any species which are calculated to be present in negative amounts are set equal to zero. The heat of reaction is summed for each of the fifteen reactions, based on the heat of formation of each component in each reaction multiplied by that reaction rate.

The change in temperature of the gas during the time increment is calculated by dividing the enthalpy change (due to chemical reaction and heat transfer) by the average heat capacity.

The above sequence is repeated three times more to generate the four Runge-Kutta coefficients used to calculate each of the weighted average rates of the fifteen reactions. The weighted average rates are then used to calculate the conditions at the end of the time increment [25]. These results are printed out and also stored in arrays for later retrieval to generate plots of the data. The program then progresses to the next time increment and successively repeats the entire Runge-Kutta loop until the time span of interest is exceeded. Conditions which also terminate calculations are exceeding the reactor length and/or calculating a negative pressure. Upon termination, the program prints out the final: pressure; mole fraction of steam; yield of any component not printed out step-by-step; Reynold's number; linear gas velocity; and the heat load in each reactor section. Approximately 20 seconds are required to calculate each complete incremental step on the Hewlett-Packard 9845-A computer.

The program stores the time, gas temperature, and gas composition at each length. Due to internal memory limitations of the HP9845-A, only 150 sets of data may be stored without the use of an external data file (e.g., a tape or disk drive). However, since the kinetic rates used in this program are

relatively slow, this memory shortage did not appear to be a problem. Typically, time steps of 5 milliseconds were specified, which resulted in smoothly changing product values. For a particularly long reactor, the analysis could be performed on separate sections of the reactor.

After the computations are completed, the operator decides whether or not to plot the results, whether to plot temperature, mole per cent, or kg/1000 kg versus reactor length, the range of values, and the pyrolysis products of interest. After the curves are plotted, the operator may enter experimental data points and label the curves from the keyboard.

SECTION 6.0

COMPARISON OF COMPUTER MODEL TO EXPERIMENTAL RESULTS

The first test, which the model should pass, involves the validation of the program to reproduce the results of the experiments used as the basis for the model. During experimentation to elucidate the flow patterns in a vortex tube, dilute propane was used as a dynamic tracer gas at 750°C [38]. One of these experiments was used to validate the hydrocarbon cracking reactions used in the pyrolysis model discussed in Section 5. The wall temperatures of the vapor cracker, in the model calculation, were adjusted by trial and error until the computed gas temperatures were within 10°C of the experimental values. The results of the model are plotted in Fig. 6-1, where it is seen that this relatively simple hydrocarbon cracking model predicted the disappearance of the dilute propane very accurately. This has important implications with respect to the agreement between this work and that reported by Van Damme [34], with regard to the temperature measurements, the gas analyses, and the ability to quench the gases during sampling. The experimental values for mol % of hydrogen, ethylene, and methane were virtually identical. The agreement between the major hydrocarbon pyrolysis products seen experimentally, and those predicted, is within about 1 mol %, which it is felt to be very acceptable. The predicted hydrogen value was about 2 mol % lower than observed experimentally, which is not in as good agreement as the other compounds.

The usefulness of the calculated kinetic expressions for predicting the pyrolysis of primary biomass vapors is shown in Fig. 6-2 for experimental Runs 55, 56, and 58, which were made last summer [12]. These runs cover the temperature range of 650 to 800°C. The wall temperatures of the vapor cracker in the model were adjusted until the calculated process stream temperatures matched those of the experimentally measured temperatures within a few degrees. The experimental data points were determined using the same assumptions as to the water of pyrolysis, the by-products of tar formation, and the conservation of mass which were used in the derivation of the kinetic rate expression for primary vapor pyrolysis [12]. As can be seen from Fig. 6-2, the predicted primary vapor values agree quite well with those deduced from the experimental data. This agreement doesn't by itself validate all of the assumptions, but there do not appear to be inconsistencies at this point of the model validation.

In Fig. 6-3, the predicted results are plotted for the formation of carbon dioxide, carbon monoxide, and hydrogen under the conditions of Run 55. The experimental data points show agreement, which is usually within 1 mol % of that predicted. Fig. 6-4 makes a similar comparison for the hydrocarbon products, with similar results. It is concluded that the concept of a prompt gas forming during the char-vapor formation, which then mixes with a secondary gas formed from the primary vapors is valid at 650°C and describes the overall phenomena quite well. Although not shown graphically, the program also predicted the experimentally observed tar formation to within 0.1% by weight.

The usefulness of the model to predict the pyrolysis products at the intermediate temperature of 730°C is shown in Fig. 6-5 for the carbon oxides and

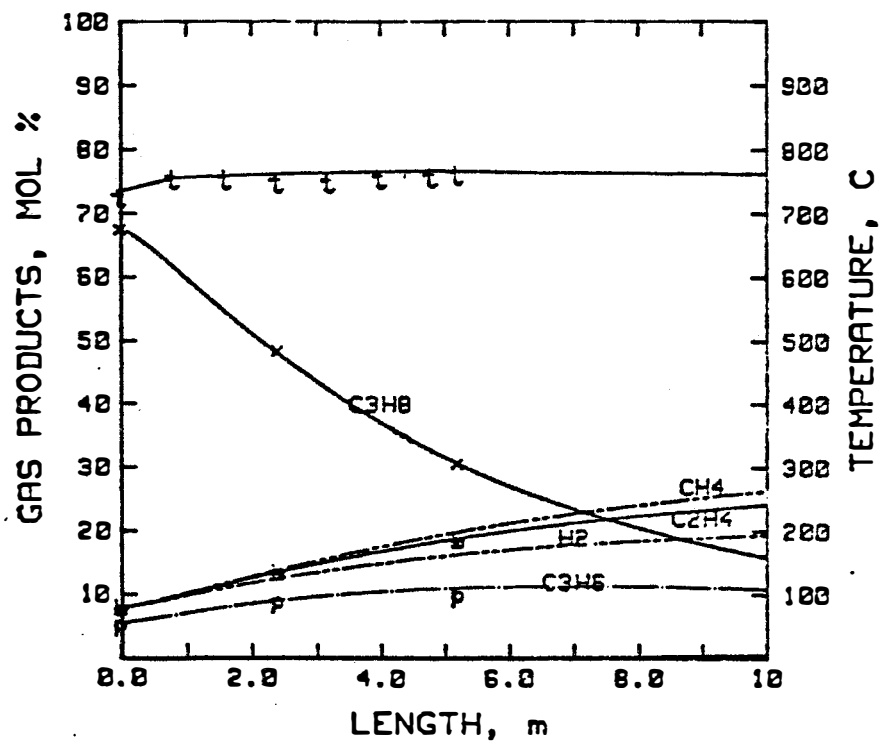


Figure 6-1. Computer Simulation of Propane Cracking (Run 25 data points)

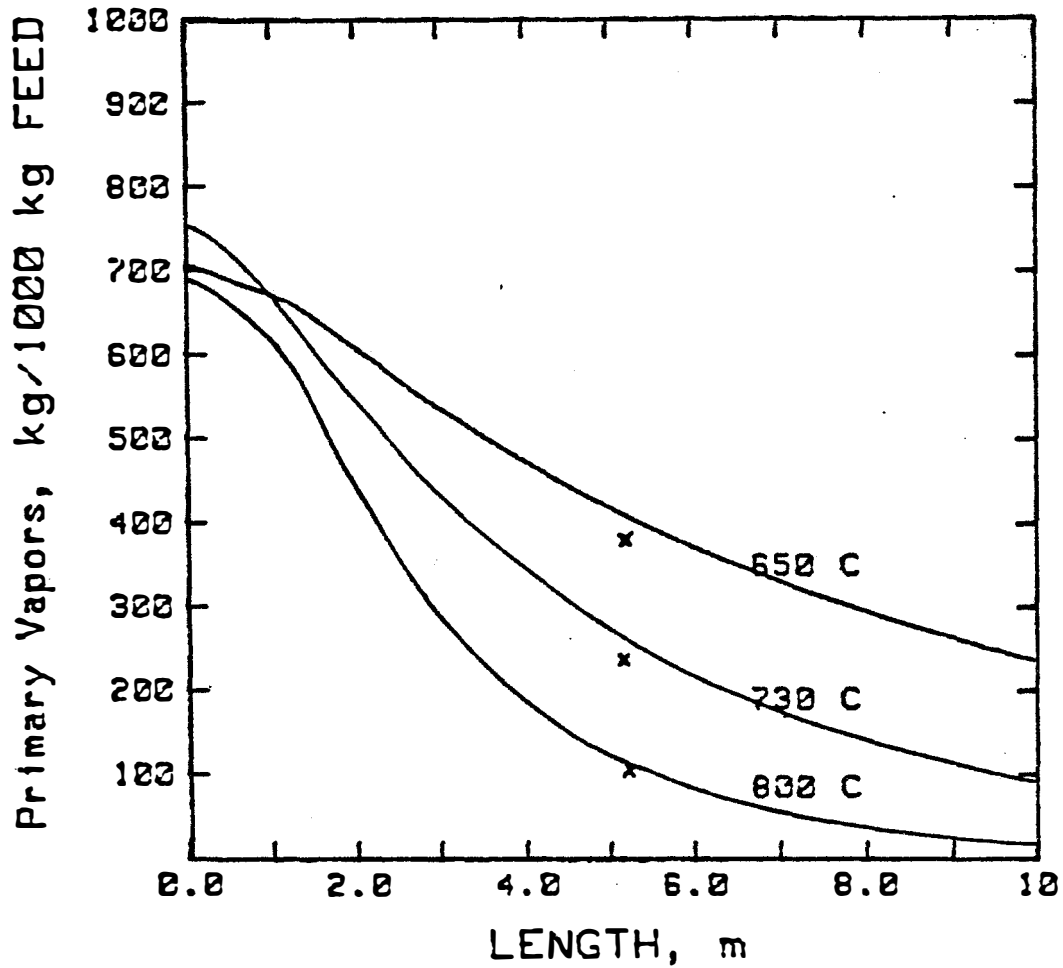


Figure 6-2. Primary Vapor Cracking Predictions for Simulated Run 55 (650°C), Run 56 (730°C), and Run 58 (800°C)

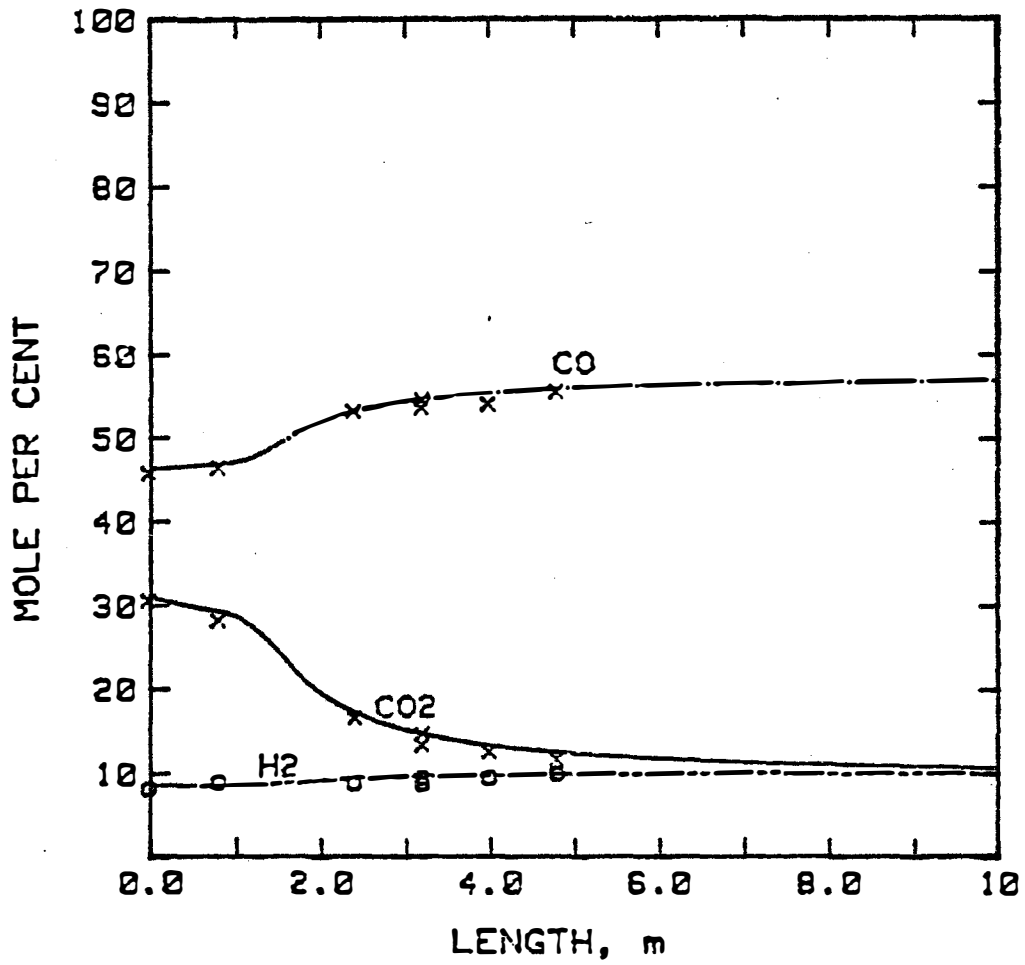


Figure 6-3. Nonhydrocarbon Gases in Simulated Run 55 (Run 55 data points)

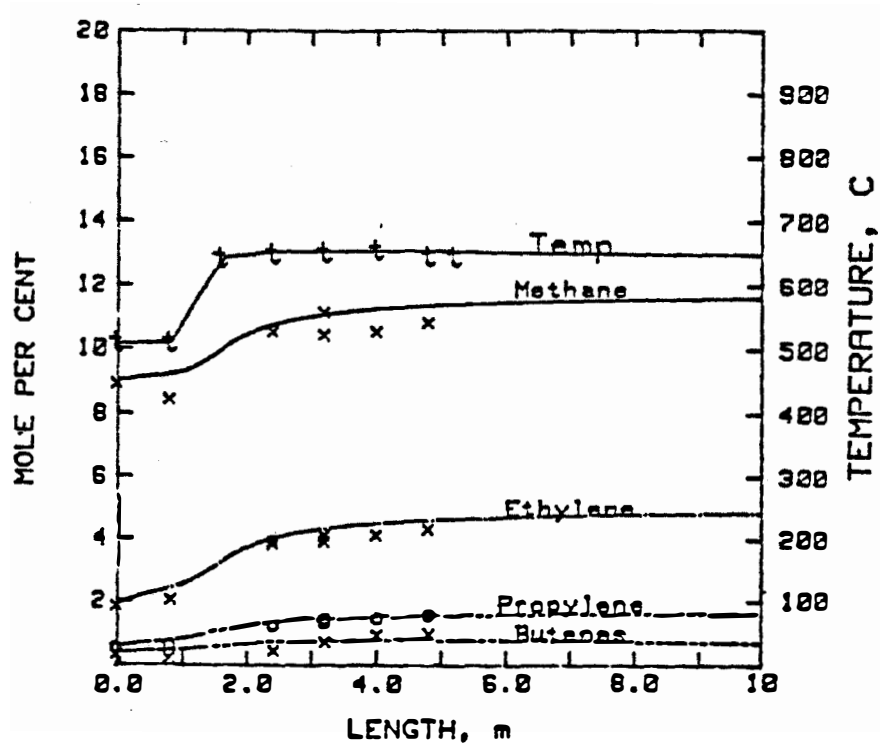


Figure 6-4. Gaseous Hydrocarbons in Simulated Run 55 (Run 55 data points)

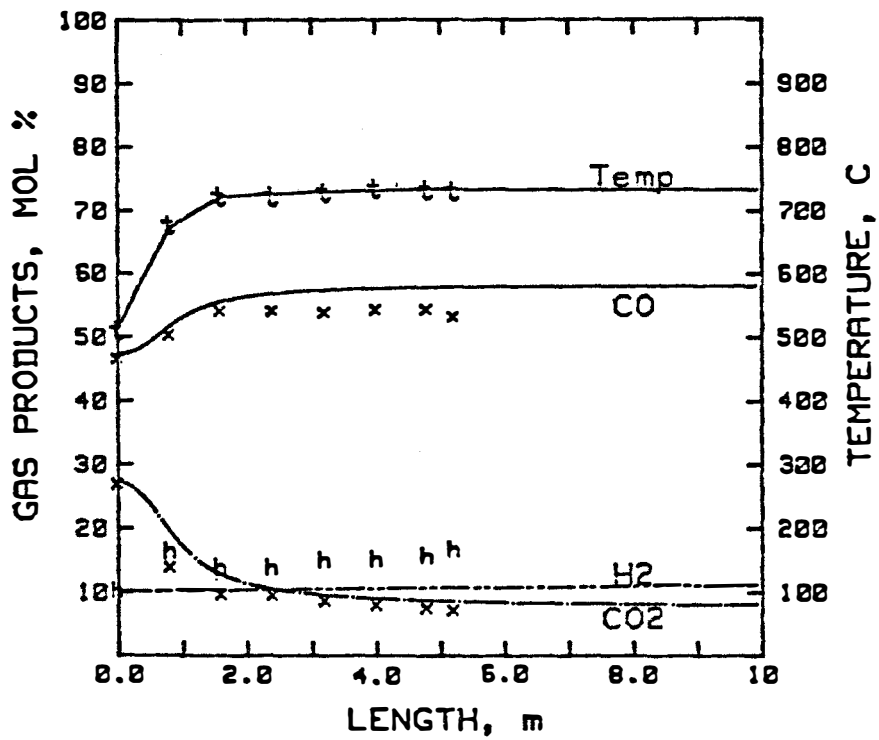


Figure 6-5. Gaseous Nonhydrocarbon in Simulated Run 56 (Run 56 data points)

Fig. 6-6 for the hydrocarbon gases. The predicted values are still seen to show the trends of the product formation, but now the carbon monoxide and the methane predictions are only within about 2 mol % of the experimental values. In Figs. 6-7 and 6-8, the same trends are seen for Run 58 at 800°C as were just described for Run 56, except that at the higher temperature the predicted values for the carbon monoxide and the methane are at slightly greater variance. The decline in the mol % of carbon dioxide occurred a bit faster experimentally than was predicted, but it asymptoted to the predicted value. This early fall in the carbon dioxide content of the gases implies that the primary vapor was cracking at a faster rate than predicted by the average gas temperature. The wall temperatures needed to raise the gas temperature at the experimentally determined rate were very high based on the convective heat transfer equation used. Vapors which had been involved in this heat transfer would have seen temperatures much higher than the bulk temperatures and would have cracked faster than if the increase in gas temperature had been accomplished with a larger surface area and a smaller temperature difference.

The wall temperature in the first section would have had to be 1175°C in order to increase the gas temperature from 511° to 679°C, if the convective heat transfer equation for turbulent flow is assumed to be valid. In order to transfer heat from the heating element to the reactor wall, the heating element must have been even hotter than the reactor wall. However, thermocouples had been installed to measure the temperature of the backside of the furnace heating elements of each furnace and none of these thermocouples tripped the alarm system set at 1050°C. Consequently, it appears that the heat transfer coefficient was considerably higher than predicted, possibly due to entrance effects and/or to a residual swirl in the gases from the cyclone separator just upstream of the vapor cracker. It has been reported [39] that in a cyclone used to heat gases, the convective heat transfer coefficient is given by

$$h = 0.042 k/D (Re)^{0.8} (Pr)^{0.4}$$

In this equation the Reynold's number is based not on the axial gas flow rate, but on the tangential gas flow rate. If the gases are swirling such that the pitch is 1.2 times the diameter [40, 41], then the tangential gas velocity would be 2.8 times the axial velocity. This would result in the swirling heat transfer coefficient being a little over four times larger than the turbulent heat transfer coefficient. This would reduce the temperature difference needed to transfer the required amount of energy by this same ratio, so that the wall temperature would be closer to 800°C than to 1175°C for the first vapor cracker section. A quick check of the calculated convective heat transfer per furnace section revealed that the heat input to the process stream did not exceed 80% of the rated furnace output in Run 58. Consequently, it is reasonable to have increased the gas temperature as much as was experimentally indicated. If the measured temperature had been higher than the true gas temperature due to radiation effects from the hot walls, the experimental carbon dioxide values would be expected to be higher than predicted due to less vapor cracking. This implies that the location of the thermocouples between the heaters served to reduce the radiation errors to a low level.

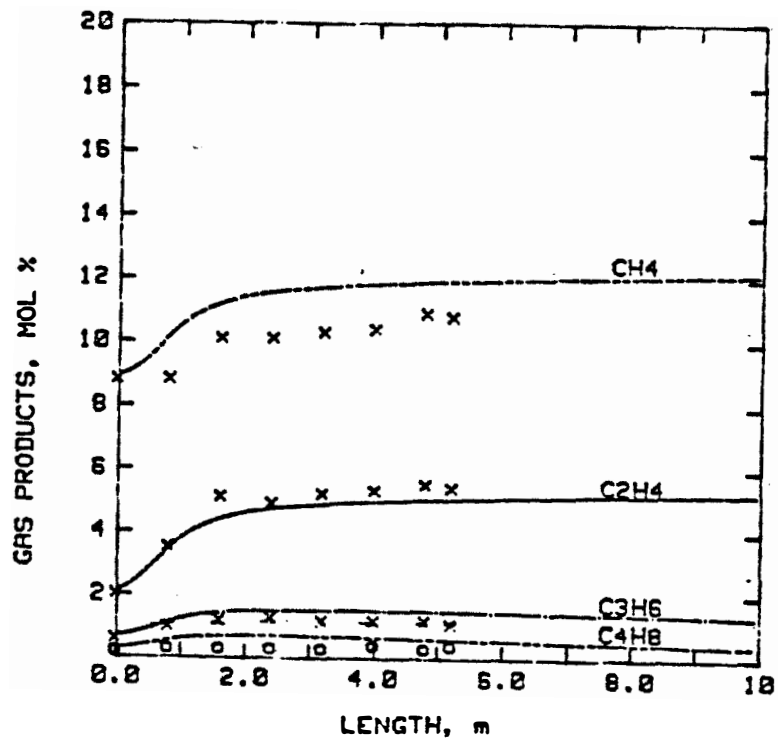


Figure 6-6. Gaseous Hydrocarbons in Simulated Run 56 (Run 56 data points)

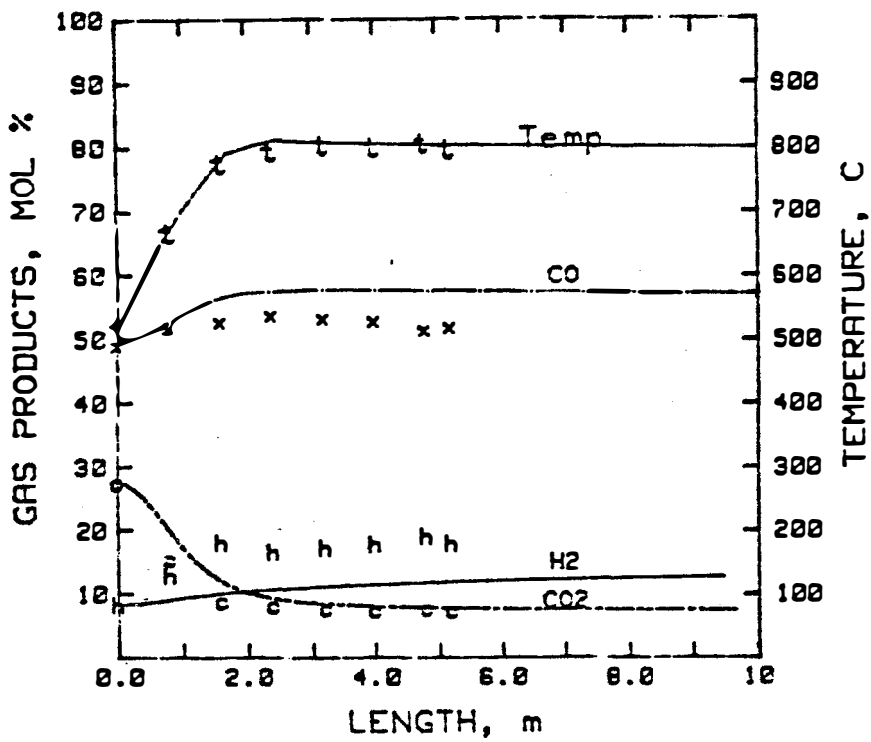


Figure 6-7. Nonhydrocarbon Gases for Simulated Run 58 (Run 58 data points)

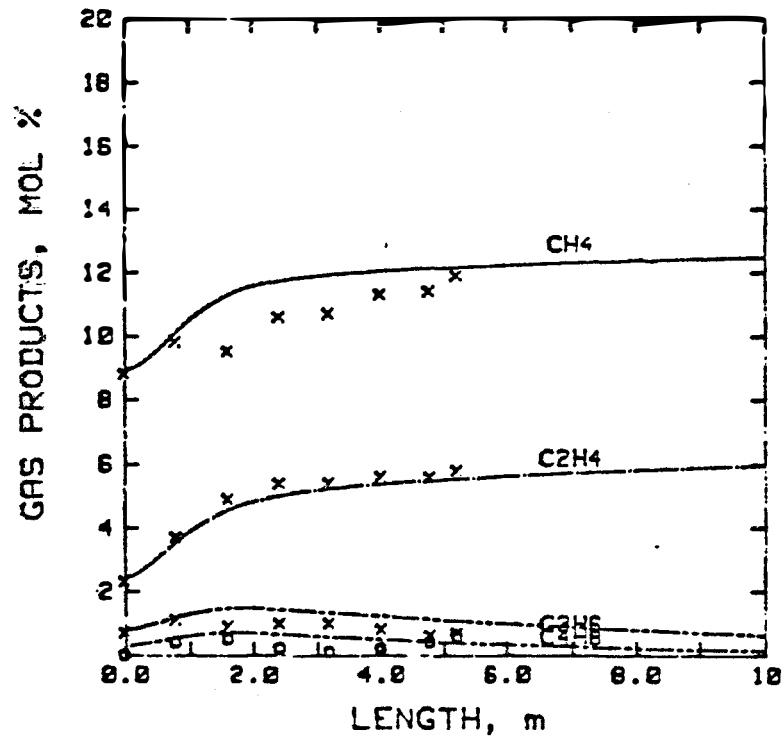


Figure 6-8. Gaseous Hydrocarbons for Simulated Run 58 (Run 58 data points)

The single, first-order global reaction assumed for tar formation is an oversimplification of a complex, multistep series of reactions [1]. (Tar is here defined as the product of dehydration and decarboxylation reactions to produce a water insoluble, polycyclic aromatic mixture having only a small amount of residual oxygen remaining.) As was reported in Ref. 12, the first-order reaction rates derived for the formation of secondary tar from the primary vapors had a negative activation energy. The effect of the negative activation energy was seen during the first attempt to run the computer program to simulate Run 55. In Run 55, the heater for the first vapor cracker section was turned off due to problems with the controller that day. This resulted in a gas temperature of 511°C at the end of the first vapor cracker. At this low temperature, the extrapolated rate for the conversion of primary vapors to secondary tars is about twice that of the extrapolated rate for vapor cracking reactions. This resulted in a predicted tar yield which was several times the experimentally observed yield. To prevent these extrapolated tar kinetics from incorrectly predicting high tar yields at the entrance of the vapor cracker, the tar cracking rate was held constant at 0.5 inverse seconds at gas temperatures below 625°C for the run simulations previously discussed. In order to determine the effect of this on the overall product slate, the tar forming kinetic rate was held constant at a value representing the average rate seen in the experimentation (0.28 inverse seconds) during a simulation of Run 58. The predicted tar yield decreased from 2.4 wt % to 2.1 wt % and the gaseous yields were essentially unchanged (the experimental tar value was 1.2 wt %).

The reason for the lack of sensitivity of the product slate to the rate of tar formation was due to the much higher rate of gas formation at the temperatures employed in Run 58. In a simulation of Run 55, setting the tar forming reaction rate at 0.28 inverse seconds would be expected to reduce the predicted tar yield from the correct value of 5.2 wt % to 2.8 wt % for a difference of 2.4 wt %. With the operational conditions of the vortex reactor close-coupled to the vapor cracker, the tar forming reaction has a very minor impact on the product slate. Unless the process stream were to have a long residence time at low temperatures prior to entering the vapor cracker, the tar forming reaction will be of little practical interest. However, if the intended use of the primary vapors is as a feedstock to a catalytic reactor at temperatures below 625°C, the thermal conversion of the primary vapors to tars would be an undesirable side-reaction, which could contribute to a fouling of the catalyst. Therefore, there may be interest in the future to establish with greater accuracy the mechanisms and reaction rates of secondary tar formation.

The ability of the model to predict the gaseous pyrolysis products was very good for the run made at 650°C. This was the run from which the secondary gas composition was calculated. However, at the higher temperatures more hydrogen and less methane, propylene and butenes were experimentally observed than were predicted. The basic assumption in the model is that the hydrocarbon reactions are completely independent of the oxygenated hydrocarbon reactions. The most widely accepted mechanisms for the pyrolysis of hydrocarbons do not involve the molecular reactions used in the model (for simplicity), but involve free radical interactions. These free radicals from the hydrocarbon pyrolysis would be expected to not only interact with themselves, but also with oxygenated hydrocarbon species. In addition, the

oxygenated hydrocarbons may be generating free radicals of their own. With the possibility of the generation of free radicals from both the oxygenated and the nonoxygenated hydrocarbons, the number of possible free radical reactions would increase dramatically. It would appear that the net result is a slight lowering in the yields of propylene and butenes and an increase in the yield of hydrogen. The nature of the products of such reactions is speculative, but would probably be water soluble species due to the tendency of oxygenated hydrocarbons to be polar in nature.

SECTION 7.0**SUMMARY**

The mathematical model for the cracking of primary biomass vapors in the vapor cracker is operational and predicts the experimentally observed vapor cracking quite well, which indicates an understanding of the global phenomena of the gas forming reactions. The model would be useful to do the preliminary design of a commercially sized vapor cracker.

A combination of reactor modifications and reinstallation of the pyrolysis system in the new facility are thought to have the potential for significant increases in throughput in the reactor, although this is of secondary importance compared to pyrolysis oil generation, quantitation, and upgrading. Recovery of pyrolysis oils, calculated to exist by mass and elemental balances, has remained elusive.

The potential is excellent for a simple process using zeolite catalysis to upgrade the primary pyrolysis oils to high octane gasoline in a single thermal step. This process would replace methanol as a feedstock with inexpensive primary pyrolysis vapors.

SECTION 8.0**FUTURE PLANS**

The upgrading of primary pyrolysis oils will continue with the MB/MS to both screen potential catalysts and to evaluate promising catalysts with a variety of process variables. The vortex reactor will be used to supply a continuous slipstream of pyrolysis vapors to a bench-scale catalytic reactor containing several hundred grams of zeolite catalyst. Initial process variable studies will use Mobil's ZSM-5 catalyst, but other promising catalysts will be evaluated after identification. The development of a pyrolysis/catalysis system intermediate in size between the MB/MS and vortex reactor will be initiated. Production and collection of a few gallons of primary pyrolysis oils will be limited to that necessary to supply the feedstock requested by Doug Elliot of PNL and N. Y. Chen of Mobil Research and Development Corporation for upgrading efforts in their laboratories. A preliminary economic evaluation will be made for the process of upgrading the primary pyrolysis oils to gasoline.

SECTION 9.0

PUBLICATIONS, PRESENTATIONS, AND FORMAL EDUCATION

Diebold successfully completed a graduate chemical engineering course in Advanced Heat Transfer. He also wrote and defended a thesis at the Colorado School of Mines entitled "The Cracking Kinetics of Depolymerized Biomass Vapors in a Continuous, Tubular Reactor." Prof. M. S. Graboski was the thesis advisor. He has now completed the requirements for and received a master of science degree in Chemical and Petroleum Refining and Engineering. Twenty-five copies of the thesis have been distributed to interested people outside of SERI in both the academic and industrial settings.

Diebold traveled to Mobil Research and Development Corp. in Paulsboro, New Jersey, to give an invited seminar on reactions of pyrolysis vapors with the 10 grams of ZSM-5, which Mobil had previously donated to the program. This seminar was in keeping with the signed cooperative agreement between Mobil and SERI. As a result of the seminar, Mobil has agreed to send SERI an additional two pounds of ZSM-5 catalyst and to share their expertise by making recommendations on SERI's screening tests with the catalyst.

The FY 1984 annual report was published as a SERI report, "Entrained-Flow, Fast Ablative Pyrolysis of Biomass, Annual Report, 1 October 1983 - 30 November 1984," SERI/PR-234-2665.

A paper has been written entitled "A Unified, Global Model for the Pyrolysis of Cellulose" and is now undergoing peer review. It is planned to submit this paper to a journal concerned with the pyrolysis of biomass.

A paper describing our progress entitled, "The Thermal and Catalytic Upgrading of Oxygenated, Primary Biomass Pyrolysis Oil Vapors," was written and presented to the 1985 Biomass Thermochemical Conversion Contractors' Meeting held in Minneapolis, Minnesota, in October 1985. The paper was published in the proceedings (PNL-SA-13571/CONF-8510167) and is available through NTIS.

A paper has been proposed to be presented at the IGT/CBETS-sponsored conference, "Energy from Biomass and Wastes X," to be held in April 1986 in Washington, D.C. The title of the paper is "Low-Pressure Upgrading of Primary Pyrolysis Oils from Biomass and Organic Wastes."

The Honorable John F. Herrington (Secretary of Energy) and Donna Fitzpatrick (Assistant Secretary for Conservation and Renewable Energy) toured the ablative pyrolysis laboratory.

SECTION 10.0

REFERENCES

1. Evans, R. J., T. A. Milne, and M. N. Soltys, 1983, "Fundamental Pyrolysis Studies," Proceedings of the 16th Biomass Thermochemical Conversion Contractor's Meeting, Portland, OR; 8-9 May 1984; Richland, WA: Battelle Pacific Northwest Laboratories.
2. Diebold, J. P., workshop chairman, 1981, Proceedings of the Specialists Workshop on the Fast Pyrolysis of Biomass; Copper Mountain, CO; 20-22 October 1980, SERI/CP-622-1096, Golden, CO: Solar Energy Research Institute.
3. Diebold, J. P., 1980, "Thermochemical Conversion of Biomass to Gasoline," Proceedings of the 11th Biomass Thermochemical Conversion Contractors Meeting, Richland, WA; 23-24 Sept. 1980, Richland, WA: Battelle Pacific Northwest Laboratories.
4. Lédé, J., Panagopoulos, J., and Villiermaux, J., 1983, "Experimental Measurement of Ablation Rate of Wood Pieces Undergoing Fast Pyrolysis by Contact with a Heated Wall," ACS Symposium on Mathematical Modeling of Biomass Pyrolysis Phenomena, 1 September 1983, Washington, DC.
5. Reed, T. B., J. Diebold, and R. Desrosiers, 1980, "Perspectives in Heat Transfer Requirements and Mechanisms for Fast Pyrolysis," Proceedings of the Specialists Workshop on the Fast Pyrolysis of Biomass, op cit.
6. Diebold, J., 1980, "Ablative Pyrolysis of Macroparticles of Biomass," Proceedings of the Specialists Workshop on the Fast Pyrolysis of Biomass, op cit.
7. Diebold, J., and J. Scahill, 1981, "Progress in the Entrained-Flow, Fast Ablative Pyrolysis of Biomass," Proceedings of the 12th Biomass Thermochemical Conversion Contractors Review Meeting; Washington, DC; 18-19 March 1981 (SERI/PR-622-1151, Golden, CO: Solar Energy Research Institute.)
8. Diebold, J. P., and J. Scahill, 1982, "Progress in the Entrained-Flow Fast Ablative Pyrolysis of Biomass, Annual Report, October 1980 to September 1981," Proceedings of the 13th Biomass Thermochemical Conversion Contractors Review Meeting; Arlington, VA; 17-19 October 1981 (SERI/PR-234-1456, Golden, CO: Solar Energy Research Institute.)
9. Diebold, J. P., and J. W. Scahill, 1984 "Ablative, Entrained-Flow Fast Pyrolysis of Biomass," Proceedings of the 16th Biomass Thermochemical Conversion Contractor's Meeting; Portland, OR; 8-9 May 1984; Richland, WA: Battelle Pacific Northwest Laboratories.

10. Diebold, J. P., and J. W. Scahill, 1983, Ablative Pyrolysis of Biomass in the Entrained-Flow Cyclonic Reactor at SERI, Annual Report, 1 October 1981 to 30 November 1982, SERI/PR-234-1883, Golden, CO: Solar Energy Research Institute.
11. Diebold, J. P., and J. W. Scahill, 1984, Entrained-Flow, Fast Ablative Pyrolysis of Biomass, Annual Report, 1 December 1982 to 30 September 1983, SERI/PR-234-2144, Golden, CO: Solar Energy Research Institute.
12. Diebold, J. P., and J. W. Scahill, 1985, Entrained-Flow, Fast Ablative Pyrolysis of Biomass, Annual Report: 1 October 1983 - 30 November 1984, SERI/PR-234-2665, Golden, CO: Solar Energy Research Institute.
13. Campbell, I. M., 1983, Biomass, Catalysts and Liquid Fuels, Technomic Pub. Co., Inc., p. 119, p. 154.
14. Chang, C. D., and Silvestri, A. J., 1977, "The Conversion of Methanol and Other O-Compounds to Hydrocarbons over Zeolite Catalysts," J. of Cat., Vol. 47, pp. 247-59.
15. Frankiewicz, T., 1980, "The Conversion of Biomass Derived Pyrolytic Vapors to Hydrocarbon," Proc. Specialists Workshop on Fast Pyrolysis of Biomass, loc. cit.
16. Milne, T. A., M. N. Soltys, and R. J. Evans, 1983, Fundamental Pyrolysis Studies Annual Report: 1 December 1982 to 30 September 1983. SERI/PR-234-2152. Golden, CO: Solar Energy Research Institute.
17. Shafizadeh, F., 1982, "Introduction to the Pyrolysis of Biomass," J. Anal. Appl. Pyrol., Vol. 3, pp. 283-305.
18. Chantal, P. et al., 1984, "Production of Hydrocarbons from Aspen Poplar Pyrolytic Oils over H-ZSM5," Applied Catalysis, Vol. 10, pp. 317-32.
19. Nisbet, H. B., 1941, "The Blending Octane Numbers of Furan and Furfuryl Alcohol," J. of Inst. Pet., 27:293.
20. Unzelman, G. H., et al., 1971, "Are There Substitutes for Lead Antiknocks," API Meeting, San Francisco, May 14, API Preprint No. 47-71.
21. Nisbet, H. B., 1946, "The Blending Octance Numbers of 2:5-Dimethyl Furan," J. of Inst. Pet., 32:162.
22. Burns, L. D., December 1984, "Organic Antiknock Chemicals," Chem. Tech., p. 744.
23. Singerman, G. M., "Methyl Aryl Ethers from Coal Liquids as Gasoline Extenders and Octane Improvers," DOE/CE/50022-1, Gulf Research and Development Company, Pittsburgh, PA.
24. Chum, H. E. et al., 1985, "Liquid Fuels from Lignins," In Biochemical Conversion Program, Semi-Annual Review Meeting, SERI/CP-231-2726, Golden, CO: Solar Energy Research Institute.

25. Mickley, H. S., T. K. Sherwood, and C. E. Reed, 1957, Applied Mathematics in Chemical Engineering, New York: McGraw-Hill, pp. 193-5.
26. Perry, R. H., editor, 1950, Chemical Engineering Handbook, 3rd Edition, New York: McGraw-Hill, pp. 370-1.
27. Katz, D. L., et al., editors, 1959, Handbook of Natural Gas Engineering, New York: McGraw-Hill, p. 169.
28. Kobe, K. A., et al., 1947-1954, "Thermochemistry for the Petrochemical Industry," Petroleum Refiner as reported by O. A. Hougan, K. E. Watson, and R. A. Ragatz (1959) in Chemical Process Principals, Part I. Material and Energy Balances, New York: John Wiley and Sons, pp. xxii-xxv.
29. Reid, R., J. Prausnitz, and T. Sherwood, 1977, The Properties of Gases and Liquids, New York: McGraw-Hill, pp. 629-77.
30. Bird, R. B., W. E. Stewart, and E. N. Lightfoot, 1960, Transport Phenomena, New York: John Wiley and Sons, p. 257.
31. Perry, R. H., and C. H. Chilton, editors, 1973, Chemical Engineering Handbook, 5th Edition, New York: McGraw-Hill, pp. 3-244.
32. Hougan, O. A., K. M. Watson, and R. A. Ragatz, 1959, Chemical Process Principles Part II. Thermodynamics, New York: John Wiley and Sons, p. 686.
33. Kreith, F., 1958, Principles of Heat Transfer, Scranton, PA: International Textbook Co., pp. 352 and 376.
34. Van Damme, P., S. Narayanan, and G. Froment, 1975, "Thermal Cracking of Propane and Propane-Propylene Mixtures: Pilot Plant Versus Industrial Data," AIChE J., Vol. 21, p. 1065.
35. Sundaram, K. M., and G. F. Froment, 1977, "Modeling of Thermal Cracking Kinetics--II. Cracking of Iso-Butane, of n-Butane, and of Mixtures of Ethane-Propane-n-Butane," Chem. Eng. Sci., Vol. 32, pp. 609-17.
36. Isbarn, G., H. J. Ederer, and K. H. Ebert, 1980, "The Thermal Decomposition of n-Hexane: Kinetics, Mechanism, and Simulation," Proceedings of the International Workshop on Modelling of Chemical Reaction Systems 1-5 September. 1981, Springer-Verlag, NY.
37. Dente, M. E., and E. M. Ranzi, 1983, "Mathematical Modeling of Hydrocarbon Pyrolysis Reactions," in Pyrolysis: Theory and Industrial Practice. Edited by L. Albright, et al., New York: Academic Press, pp. 133-73.
38. Diebold, J. P., and J. W. Scahill, 1984, "Ablative Pyrolysis of Biomass to Olefins and Aromatic Liquids in a Vortex Reactor," AIChE Winter National Meeting, 11-14 March 1984, Paper 31d.

39. Szekely, J., and R. Carr, 1966, "Heat Transfer in a Cyclone," Chem. Eng. Sci., Vol. 21, pp. 1119-32.
40. Diebold, J. P., and J. W. Scahill, 1981, Progress in the Entrained-Flow, Fast Ablative Pyrolysis of Biomass, Annual Report, Oct. 1980 to Sept. 1981, SERI/PR-234-1456, Golden, CO: Solar Energy Research Institute, p. 17.
41. Hartnett, J., and E. Eckert, 1957, "Experimental Study of the Velocity and Temperature Distribution in a High-Velocity Vortex-Type Flow," Trans ASME, May, pp. 751-8.

ABSTRACT

The ablative, fast pyrolysis system was relocated to SERI's new, permanent Field Test Laboratory. Pyrolysis system modifications were made to increase the energy available to the vortex reactor and to enhance the collection efficiency of primary pyrolysis vapors. Mathematical modeling of the vapor cracker has resulted in the ability to accurately predict experimental results with respect to the thermal cracking of the primary vapors, the generation of noncondensable gases, and the gas composition. The computer algorithm of this model can be readily used to perform experimental simulation and/or reactor scale-up due to its fundamental nature. Preliminary screening tests with pure ZSM-5 zeolite catalyst, supplied by Mobil Research and Development Corporation, have shown promise for the conversion of primary pyrolysis oil vapors to aromatic hydrocarbons; i.e., gasoline.

Document Control Page	1. SERI Report No. SERI/PR-234-3012	2. NTIS Accession No.	3. Recipient's Accession No.
4. Title and Subtitle Entrained-Flow, Fast Ablative Pyrolysis of Biomass		5. Publication Date December 1986	
7. Author(s) James P. Diebold, John W. Scahill, Robert J. Evans		8. Performing Organization Rept. No.	
9. Performing Organization Name and Address Solar Energy Research Institute 1617 Cole Blvd. Golden, CO 80401		10. Project/Task/Work Unit No. 7540.10	
		11. Contract (C) or Grant (G) No. (C) (G)	
12. Sponsoring Organization Name and Address		13. Type of Report & Period Covered Annual Report/12-1-84 - 12-31-85	
		14.	
15. Supplementary Notes			
16. Abstract (Limit: 200 words) <p>The ablative, fast pyrolysis system was relocated to SERI's new, permanent Field Test Laboratory. Pyrolysis system modifications were made to increase the energy available to the vortex reactor and to enhance the collection efficiency of primary pyrolysis vapors. Mathematical modeling of the vapor cracker has resulted in the ability to accurately predict experimental results with respect to the thermal cracking of the primary vapors, the generation of noncondensable gases, and the gas composition. The computer algorithm of this model can be readily used to perform experimental simulation and/or reactor scale-up due to its fundamental nature. Preliminary screening tests with pure ZSM-5 zeolite catalyst, supplied by Mobil Research and Development Corporation, have shown promise for the conversion of primary pyrolysis oil vapors to aromatic hydrocarbons; i.e., gasoline.</p>			
17. Document Analysis			
a. Descriptors			
b. Identifiers/Open-Ended Terms			
c. UC Categories			
18. Availability Statement		19. No. of Pages	
		20. Price	